REPORT NO. NADC-82025-60

DESIGN AND DEVELOPMENT OF AN AUTOMATICALLY CONTROLLED VARIABLE-LOAD ENERGY ABSORBER

James C. Warrick and Joseph W. Coltman
SIMULA INC.
2223 S. 48th Street
Tempe, AZ 85282

MARCH 1984

FINAL REPORT
P.E. 62241N
AIRTASK NO. WF41-451-403

Approved For Public Release; Distribution Unlimited

Prepared For
NAVAL AIR SYSTEMS COMMAND
Department of the Navy
Washington, DC 20361

NOTICES

REPORT NUMBERING SYSTEM – The numbering of technical project reports issued by the Naval Air Development Center is arranged for specific identification purposes. Each number consists of the Center acronym, the calendar year in which the number was assigned, the sequence number of the report within the specific calendar year, and the official 2-digit correspondence code of the Command Office or the Functional Directorate responsible for the report. For example: Report No. NADC-78015-20 indicates the fifteenth Center report for the year 1978, and prepared by the Systems Directorate. The numerical codes are as follows:

CODE	OFFICE OR DIRECTORATE
00	Commander, Naval Air Development Center
01	Technical Director, Naval Air Development Center
02	Comptroller
10	Directorate Command Projects
20	Systems Directorate
30	Sensors & Avionics Technology Directorate
40	Communication & Navigation Technology Directorate
50	Software Computer Directorate
60	Aircraft & Crew Systems Technology Directorate
70	Planning Assessment Resources
80	Engineering Support Group

PRODUCT ENDORSEMENT – The discussion or instructions concerning commercial products herein do not constitute an endorsement by the Government nor do they convey or imply the license or right to use such products.

TECHNICAL MONITOR - The technical monitor for this program was Mr. L. Domzalski of the Seating and Escape Branch, Life Support Engineering Division, Aircraft and Crew Systems Technology Directorate.

APPROVED BY: _____ DATE: 15 May 1984

T. J. GALLAGHER
CAPT, MSC, USN

UNCLASSIFIED

SECURITY CLASSIFICATION OF THIS PAGE (When Data Entered)

REPORT DOCUMENTATION PAGE	READ INSTRUCTIONS BEFORE COMPLETING FORM
1. REPORT NUMBER: NADC-82025-60	2. GOVT ACCESSION NO.: AD-A142 683
	3. RECIPIENT'S CATALOG NUMBER:
4. TITLE (and Subtitle): DESIGN AND DEVELOPMENT OF AN AUTOMATICALLY CONTROLLED VARIABLE-LOAD ENERGY ABSORBER	5. TYPE OF REPORT & PERIOD COVERED: FINAL REPORT
	6. PERFORMING ORG. REPORT NUMBER: TR-83423
7. AUTHOR(s): James C. Warrick, Joseph W. Coltman	8. CONTRACT OR GRANT NUMBER(s): N62269-82-C-0254
9. PERFORMING ORGANIZATION NAME AND ADDRESS: Simula Inc., 2223 S. 48th Street, Tempe, AZ 85282	10. PROGRAM ELEMENT, PROJECT, TASK AREA & WORK UNIT NUMBERS: P.E. 62241N, AIRTASK WF41-451-403
11. CONTROLLING OFFICE NAME AND ADDRESS: Naval Air Development Center, Aircraft & Crew Systems Technology Directorate, Warminster, PA 18974	12. REPORT DATE: March 1984
	13. NUMBER OF PAGES: 67
14. MONITORING AGENCY NAME & ADDRESS (if different from Controlling Office): Naval Air Systems Command (Air-310H), Washington, D.C. 20361	15. SECURITY CLASS. (of this report): UNCLASSIFIED
	15a. DECLASSIFICATION DOWNGRADING SCHEDULE

16. DISTRIBUTION STATEMENT (of this Report)

Approved for public release; distribution unlimited.

17. DISTRIBUTION STATEMENT (of the abstract entered in Block 20, if different from Report)

18. SUPPLEMENTARY NOTES

19. KEY WORDS (Continue on reverse side if necessary and identify by block number)

Variable-Load Energy Absorber	Computer Models	Human Tolerance
Load-Limiting Device	Energy Absorbers	Spinal Injury
Aircraft Crashworthiness	Dynamic Testing	
Aircraft Seats	MAVLEA	
Hydraulic Valve	ASAVLEA	

20. ABSTRACT (Continue on reverse side if necessary and identify by block number)

The feasibility of an automatically controlled variable-load hydraulic energy absorber for use in crashworthy seating systems was investigated. In contrast to other systems, this model contained an acceleration-sensing device capable of automatic control to compensate for differences in occupant weight. A series of dynamic crash tests were performed in which the hardware successfully decelerated weights representing those of the 5th- through 95th-percentile occupants to a predetermined constant acceleration. The

DD FORM 1 JAN 73 1473 EDITION OF 1 NOV 65 IS OBSOLETE

UNCLASSIFIED

SECURITY CLASSIFICATION OF THIS PAGE (When Data Entered)

system was also compared to a previously developed variable-load energy absorber system in terms of size, weight, cost, reliability, and accuracy. The program concluded that the automatically controlled variable-load energy absorber is capable of providing a predetermined constant deceleration, but recommends further testing with human surrogates to verify the capability of properly protecting human occupants from spinal injury.

TABLE OF CONTENTS

TABLE OF CONTENTS (CONTD)

LIST OF ILLUSTRATIONS

LIST OF ILLUSTRATIONS (CONTD)

LIST OF TABLES

INTRODUCTION

The low tolerance of the human spine to compressive loading is recognized as a major factor in severe injuries suffered during helicopter crashes. Consequently, the seats of most new U.S. military helicopters are required to use vertical energy absorbers (load-limiters) to limit spinal load to a tolerable level.

Because spinal load cannot be measured conveniently, and seat bucket acceleration can, the criteria for energy-absorbing seats have evolved using seat bucket acceleration as the primary indicator. To maintain some predetermined optimum seat bucket acceleration, a seat's load limiters should be adjustable in order to compensate for differences in occupant weight. Such load limiters are called variable-load energy absorbers, and can be designed in many different ways to achieve adjustability. Previous development has emphasized methods whereby the occupant must manually select an appropriate energy absorber load by adjusting a dial. The potential for error or neglect makes such methods less than ideal.

The research reported herein investigated the feasibility of an automatically controlled variable-load energy absorber, which would require no attention whatsoever from the seat occupant. Specifically, the investigated device consists of a hydraulic cylinder equipped with an acceleration-sensing pressure relief valve. In operation, the load required to elongate the hydraulic cylinder is proportional to the fluid pressure, which is regulated by the relief valve, which in turn is governed by the acceleration sensor.

The following sections of this report describe the development, fabrication, and testing of the automatically controlled variable-load energy absorber, and evaluate it relative to existing manually adjustable variable-load energy absorbers:

- Definition of terms
- Requirements
- Concept Description
- Development
- Description of Test Article
- Dynamic Testing
- Alternate Configuration
- Comparison of ASAVLEA to MAVLEA
- Conclusions and Recommendations.

DEFINITION OF TERMS

The following text defines key words that might not be familiar to the reader.

Acceleration or Deceleration

Synonymous terms denoting rate of change of velocity.

ASAVLEA

Acceleration-sensing automatic variable-load energy absorber.

Companion Energy Absorber

In a variable-load energy-absorbing system, the total limit load may be the sum of the loads from two sources, one source being a fixed-load primary energy absorber, the other being a variable-load energy absorber. In such a case, the fixed-load energy absorber is said to be the companion of the variable-load energy absorber.

Energy Absorber (E/A), Load Limiter, Load-Limiting Device, Attenuator

These are interchangeable names of devices used to limit the load in a structure to a preselected value. These devices absorb energy without significant elastic rebound by providing a resistive force applied over a deformation distance.

FLEA

Fixed-load energy absorber.

ft/sec

Feet per second.

gal/min

Gallons per minute.

Limit Load

Limit load refers to the load a structure will carry before yielding. Similarly, in an energy-absorbing device, it represents the load at which the device deforms in performing its function.

MAVLEA

Manually adjustable variable-load energy absorber.

msec

A millisecond equals 0.001 second.

Occupant Vertical Effective Weight

This is the portion of occupant weight supported by the seat with the occupant seated in a normal flight position. The vertical effective weight is considered to be 80 percent of the occupant weight, plus equipment and clothes carried above the knees. The weight of the feet, boots, lower legs, and part of the thighs is carried directly by the floor through the feet.

Variable-Load Energy Absorber

An energy absorber with the capability of varying the limit load at which it deforms.

REQUIREMENTS

Foremost, Simula was to analyze, design, fabricate, and test a breadboard model of the acceleration-sensing automatic variable-load energy absorber (ASAVLEA) to demonstrate its feasibility for limiting crash accelerations to human tolerance levels. Dynamic performance of the device during the crash conditions was therefore of primary importance.

Other constraints applied to the design were simplicity, reliability, and cost effectiveness. The breadboard model was not required to have the compactness of a production design; it was ruggedly made to endure repeated testing, with easily accessible parts for replacement or adjustment.

Of all the design criteria, the most obvious is that the ASAVLEA must provide the correct predetermined deceleration for any occupant weight from the 5th- to the 95th-percentile. The weight of equipment sometimes carried by the crewmember is also a significant variable. Therefore, Simula chose to make the energy absorbers operate between the range of the lightly clad 5th- to the heavily equipped 95th-percentile occupant.

The movable weight of the seat (including not only the seat bucket, but also cushions, restraints, adjustment mechanisms, bearings, headrest, etc.) is another factor affecting the load requirements of the energy-absorbing system. The weight of these items is fixed, and therefore the load decelerating the bucket can be provided by the fixed-load energy absorber. The effect of bucket weight on the total system is still very important. A lightweight bucket allows occupant weight variations to have large effects on the total movable weight, and thus causes the highest percentage of total load to be provided by the ASAVLEA. Therefore, this development emphasized the conditions occurring in a lightweight seat such as the Navy's SH-60B Seahawk, the bucket of which (with accessories) weighs 23 lb. Other, heavier, buckets were also evaluated: a 60-lb bucket and a 110-lb bucket similar to UH-60A Black Hawk and AH-64A Apache buckets, respectively. Table 1 summarizes the seat bucket and occupant effective weights for which the automatically controlled energy-absorbing test hardware was designed to accommodate.

To enhance reliability by providing redundancy, the ASAVLEA was planned to operate in parallel with a fixed-load energy absorber, one of each per seat. The fixed-load energy absorber was sized to provide as much load as possible,

TABLE 1. EFFECTIVE WEIGHT OF CREWMEMBERS AND SEAT BUCKET

Item	Lightly Equipped 5th-percentile (lb)	Heavily Equipped 95th-percentile (lb)
Occupant	136.5	212.0
80 Percent of Occupant	109.2	169.6
Clothing	3.5	9.75
80 Percent of Clothing	2.8	7.8
Helmet and Equipment	0.0	22.6
Crewmember Effective Weight	112.0	200.0
Lightweight Seat Bucket	23.0	23.0
Total Movable Weight	135.0	223.0

without exceeding that required by the 5th-percentile occupant. Additional load for heavier occupants would be provided by the ASAVLEA. As discussed in the "Development" section, the ASAVLEA must discharge a maximum of 75 gal/min through its relief valve. For a reasonably compact relief valve, approximately 400 psi of pressure drop was expected to occur, even with the relief valve wide open. Therefore, the fixed-load energy absorber was downsized accordingly to compensate for the inability of the hydraulic energy absorber to achieve zero load at high rates of elongation.

The ASAVLEA was sized for crash conditions equal to the 95th-percentile survivable crash, i.e., Dynamic Test Number 1 of MIL-S-81771A (Reference 1). In this test the energy absorber is expected to stroke 10 to 12 in. and reach an elongation rate of 25 ft/sec. The ASAVLEA was to respond to a crash acceleration onset rate of up to 2,100 G/sec without overshooting the attenuated acceleration set-point by an intolerable amount.

Rather than the 11.5 G recommended by TR-79-22D (Reference 2), the attenuated acceleration set point was chosen to be 14.5 G, identical to the earlier recommended set point of TR-71-22 (Reference 3). The Army, without benefit of more definitive data, decided that 14.5 G was too high, and reduced the criteria for TR-79-22D to 11.5 G for the 50th-percentile occupant. Since the Army reduced the set point, several crashes have occurred of UH-60A Black Hawk helicopters equipped with Simula seats with the fixed-load energy absorbers set to 14.5 G for the 50th-percentile occupant. The occupants' spines were protected by the energy absorbers in each case where there was no exceptional event, such as one incident where the protrusion of a tree limb into the cockpit damaged the seat. Thus, field experience indicates that limit loads set for the effective weight of the 50th-percentile occupant decelerated at 14.5 G is an appropriate target value for energy absorbers used in these military applications.

Candidate hydraulic fluids were also sought. Specifications of fluid properties were demanding, and included the following:

- Useful temperature range of -60 to + 160°F
- Ten-year life in a sealed system
- Nonflammability
- Low viscosity
- High viscosity index, i.e., viscosity relatively unaffected by temperature.

The hydraulic energy absorber was required to be reliable and to incorporate as many fail-safe and redundant features as was consistent with cost constraints. Among the features evaluated were filters and redundant pressure-relief valves.

Cost was to be minimized by avoiding complexity and by using standard materials and conventional processes. If the hydraulic energy absorber were to be consistent with fixed-load inversion tube energy absorbers, no maintenance would be required, and no deleterious effects could be expected from temperature extremes, vibration, or exposure to contaminants.

Simula chose a target accuracy for the ASAVLEA of ±2 G, including all effects with the exception of temporary overshoot.

The contract Statement of Work required that the breadboard ASAVLEA model be built and dynamically tested with rigid masses representing the weights of the 5th- through 95th-percentile occupants. Another condition, called the distributed mass condition, was also to be evaluated using a computer model simulating the flexibilities of an occupant and seat to provide a comparative analysis of occupant response to a constant acceleration function versus a constant force function.

CONCEPT DESCRIPTION

The ASAVLEA is essentially a hydraulic shock absorber, and elongation is resisted by pressure generated from fluid passing through a relief valve. The relief valve must automatically restrict the flow to whatever degree is necessary to provide 14.5-G deceleration. The overall concept is shown schematically in Figure 1, and the operation of the relief valve is illustrated in Figure 2 and described in the following paragraphs.

Relief Valve Operation

The relief valve may be described as a two-stage servo valve. In the 1st stage, acceleration is detected by the forces acting on a small mass, called the G-sensing mass. The tiny forces and motions of the G-sensing mass are then amplified and used to control the 2nd stage valve. If it were not for the amplification in the two-stage concept, the G-sensing mass would need to be prohibitively heavy.

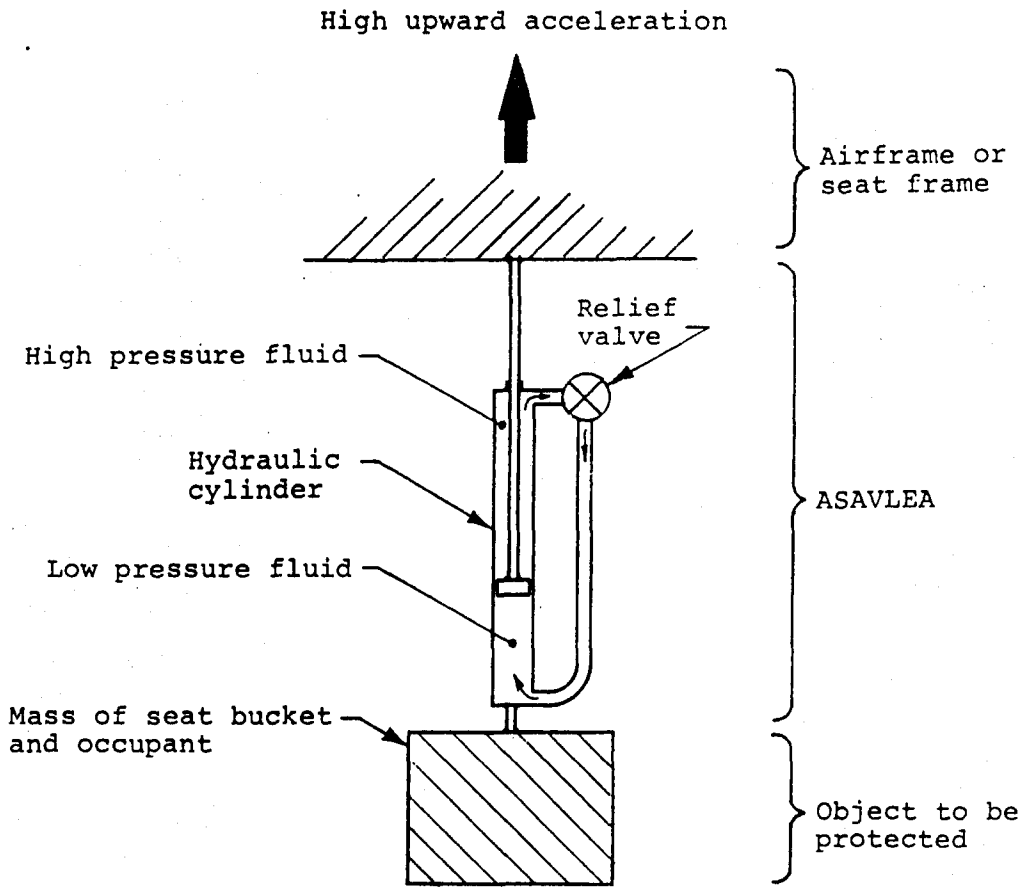

Figure 1. Position of ASAVLEA between airframe and protected mass.

The power for the amplification comes from fluid bypassed around the 2nd stage valve to the 1st stage chamber. It can be seen in Figure 2 that the 2nd stage valve spool position is dependent upon the amount of fluid in the 1st stage chamber. To change the amount of fluid in the 1st stage chamber (thus, the position of the 2nd stage valve) incoming metered fluid can be selectively discharged. The functions of the various components may be best understood by comparing the cause and effect relationships at two conditions: equilibrium and disequilibrium.

At equilibrium the following conditions exist:

- The pressure in the high-pressure end of the cylinder is correct to deliver 14.5-G deceleration to the mass to which the cylinder is connected.

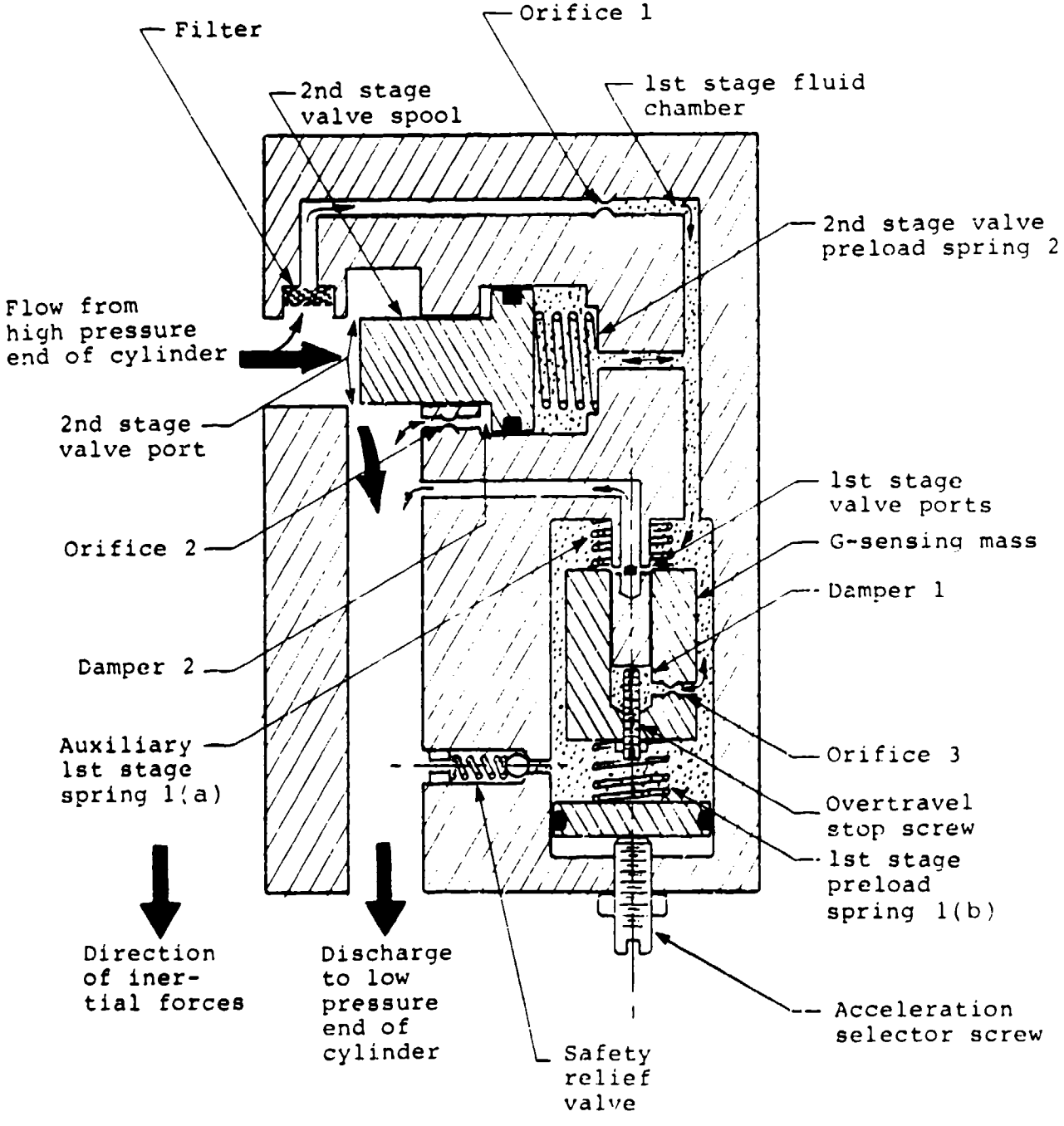

Figure 2. Relief valve schematic.

- The downward inertial load of the G-sensing mass is exactly balanced by the net upload from preload springs 1(a) and 1(b). This occurs at one unique condition precalibrated by the G-level adjustment screw.

- The 1st stage valve, (connected to the G-sensing mass), is open to the degree necessary to discharge fluid at the exact rate fluid is entering through orifice 1.

- Therefore, no net change of fluid volume in the 1st stage chamber occurs, and no movement of the 2nd stage valve spool results.

Now consider the case of disequilibrium, when, due to some external condition, the acceleration temporarily falls to a value less than 14.5 G. The following sequence occurs to restore equilibrium:

- The G-sensing mass, no longer pressed downward by the full 14.5-G inertial load, is displaced slightly upward by the load from the preload spring.

- This closes the 1st stage valve to a degree less than its equilibrium condition, and therefore reduces the rate of fluid discharged from the 1st stage.

- Fluid begins to accumulate in the first stage chamber and therefore displaces the 2nd stage valve spool to the left.

- As the movement of the 2nd stage spool continues, the 2nd stage valve gradually closes, progressively restricting the fluid flow, and therefore increasing the pressure in the high pressure side of the hydraulic cylinder.

- When the cylinder pressure reaches the magnitude such that 14.5-G deceleration is restored, the G-sensing mass returns to its equilibrium position, causing the 2nd stage valve to halt its movement.

- Equilibrium is thus restored at the new position of the 2nd stage valve.

Notice that the 2nd stage spool is held in a somewhat tenuous balance between the pressure forces on its ends. The areas on its ends were chosen to cause the pressure on its right side to be about one half of that on the left side. This enables the pressure drops across orifice 1 and the 1st stage valve to be equal, resulting in symmetrical restoration action either above or below 14.5 G. Actually, a concession was made to the availability of standard components, which resulted in the 1st stage equilibrium pressure being 44 percent of the cylinder pressure, with little degradation of symmetry.

A feature which helps maintain stability of the 2nd stage valve is labeled "Damper 2" (Figure 2). Fluid surging through orifice 2 dampens the motion of the 2nd stage valve. Similarly, the motion of the G-sensing mass is dampened by fluid surging through orifice 3 into and out of damper chamber 1.

The 2nd stage valve preload spring (spring 2) serves only to hold the 2nd stage valve closed prior to the crash pulse. For proper function, the 2nd stage

valve must start closed, then progressively open as the fluid discharge rate increases.

Springs 1(a) and 1(b) hold the 1st stage valve closed prior to the crash pulse. If it were not for the overtravel stop screw, the springs would push the valve far past the closed position. The overtravel stop screw permits the motion of the 1st stage valve to be halted just beyond (approximately 0.001 in.) the fully closed position. This feature reduces the time lag of the initial G-sensing mass response.

Due to the preload of spring 1(a) and the presence of the overtravel stop screw, the first stage valve does not begin to open until approximately 11 G is experienced. Then, if the acceleration continues to rise, the valve only has to move approximately 0.003 in. to reach its equilibrium condition at 14.5 G. This motion must be small, in order to preserve a sufficiently high frequency response of the 1st stage. The 2nd stage valve, on the other hand, does not require such rapid response, but may open as much as 0.10 in. to discharge large quantities of fluid.

Also note that the forces acting upon the G-sensing mass are measured in ounces, while those acting upon the 2nd stage valve are measured in hundreds of pounds. This is perhaps the most important reason that the two-stage approach was adopted.

Reliability Features

Safety features include the filter upstream from orifice 1 and the safety relief valve. The filter prevents contaminants from clogging the tiny passages of orifice 1 or the 1st stage valve.

The safety relief valve is located where it is on Figure 2 because the flow through the 1st stage is only about 0.5 gal/min, while that through the 2nd stage may be as high as 75 gal/min. The safety relief valve can therefore be very small and compact, in comparison to the 2nd stage valve. The pressure in the 1st stage chamber is always about 44 percent of that in the cylinder, thus the safety valve can have the desired ultimate effect upon the cylinder pressure.

Another reliability feature results from the use of the ASAVLEA in parallel with a fixed-load energy absorber. This causes an improvement in the fail-safe conditions during both operational and crash loading. Further explanation of the fail-safe conditions may be found in the "Reliability Comparison" section.

DEVELOPMENT

The acceleration-sensing automatic variable-load energy absorber (ASAVLEA) was developed by an iterative process, beginning with rough hand calculation and followed by progressive refinement through the use of a computer model. The computer model contained representations of the detailed components of the hydraulic pressure relief valve in order to simulate the transient dynamic response of the system. This enabled prediction of performance and optimization of parameters affecting dynamic performance.

In addition to dynamic performance, other requirements listed in the "Requirements" section of this report were also considered. The following text describes the methods used to develop the concept into successful hardware, and discusses some choices and alternatives.

ASAVLEA Computer Model

A computer model was developed to simulate the response of the ASAVLEA under dynamic conditions. The modular model was used in conjunction with two types of occupant models: the lumped mass model, and five degree-of-freedom distributed mass model (Figure 3). In each case the provision was made to incorporate a fixed-load energy absorber (FLEA) in parallel with the ASAVLEA. The dynamic rate sensitivity of the FLEA is simulated by the damper accompanying the fixed-load energy absorber.

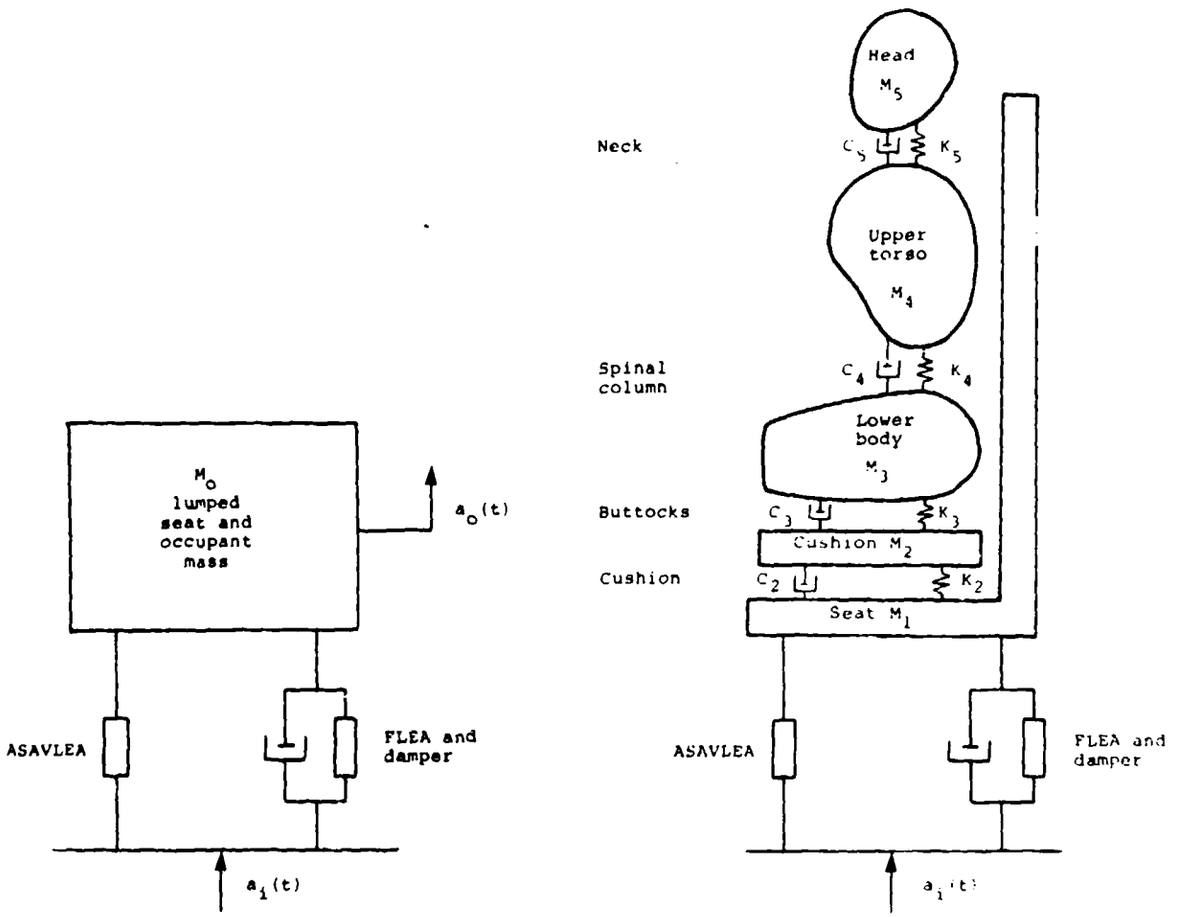

a. Lumped mass system.

b. Distributed mass system.

Figure 3. Seat/occupant system models utilizing the ASAVLEA computer model.

The ASAVLEA computer model utilizes fifteen nonlinear fluid flow equations which govern the flow and pressures throughout the device. Each equation is based on incompressible fluid mechanics theory, although the compressibility of the main chamber fluid column was modeled as an additional degree-of-freedom for the computer simulation (i.e. spring in series with the ASAVLEA). Figure 4 shows features within the automatic relief valve which were included in the computer model. The moving segments within the relief valve of the ASAVLEA were treated as rigid bodies acting under the influence of the inertial, pressure, and spring forces.

The flow coefficients used in the flow equations are nonlinear functions of the local Reynold's Number. However, within the fluid velocity range seen in the dynamic simulations, it was found that the coefficients were essentially constant.

Fluidic impulsive forces due to change of direction of the fluid at the valve/valve port interface were treated in the force balance of the 1st stage valve. Continuity equations ensure that the displaced volume due to the moving valve segments is consistent with the fluid flow. The equations governing fluid mechanics within the energy absorber consider losses due to expansion, contraction, and orifice flow.

The equations of motion for the masses and the occupant segments are solved using an Adams-Moulton predictor corrector technique. Since this technique is not self-starting, a Runge-Kutta method was incorporated into the algorithm. The algorithm had the capability of integrating with variable step sizes to increase the speed of integration while maintaining the specified error bounds between the predictor and corrector steps. However, the solution of the pressure and flow rate equations in conjunction with the equations of motion necessitated fixed-time step integration.

The integration algorithm for the equations of motion requires that first and second derivatives of the displacement parameters be evaluated at intermediate points. The second derivatives, or accelerations, were derived from a balance of the following forces acting on the masses: fluid pressure, momentum change, spring, and damper. Therefore, at each intermediate step the integration subroutine called another subroutine which solved simultaneously the pressure and flow rate equations to obtain the instantaneous second derivatives. As noted above, the fluid flow equations were nonlinear, with the difference in pressure, ΔP, being proportional to the square of the local fluid velocity. These equations were linearized using a technique derived for this program. There are general methods for linearizing this type of equation; however, the cost and time required for their implementation would have been prohibitive under this contract.

The linearization technique utilized past values of local fluid pressure differences, since it was expected that these pressure differences would change relatively slowly. As an example, consider the equation governing flow through a sharp-edged orifice:

$$P_1 - P_2 = \frac{\rho Q_0^2}{2C_0^2 A_0^2}$$

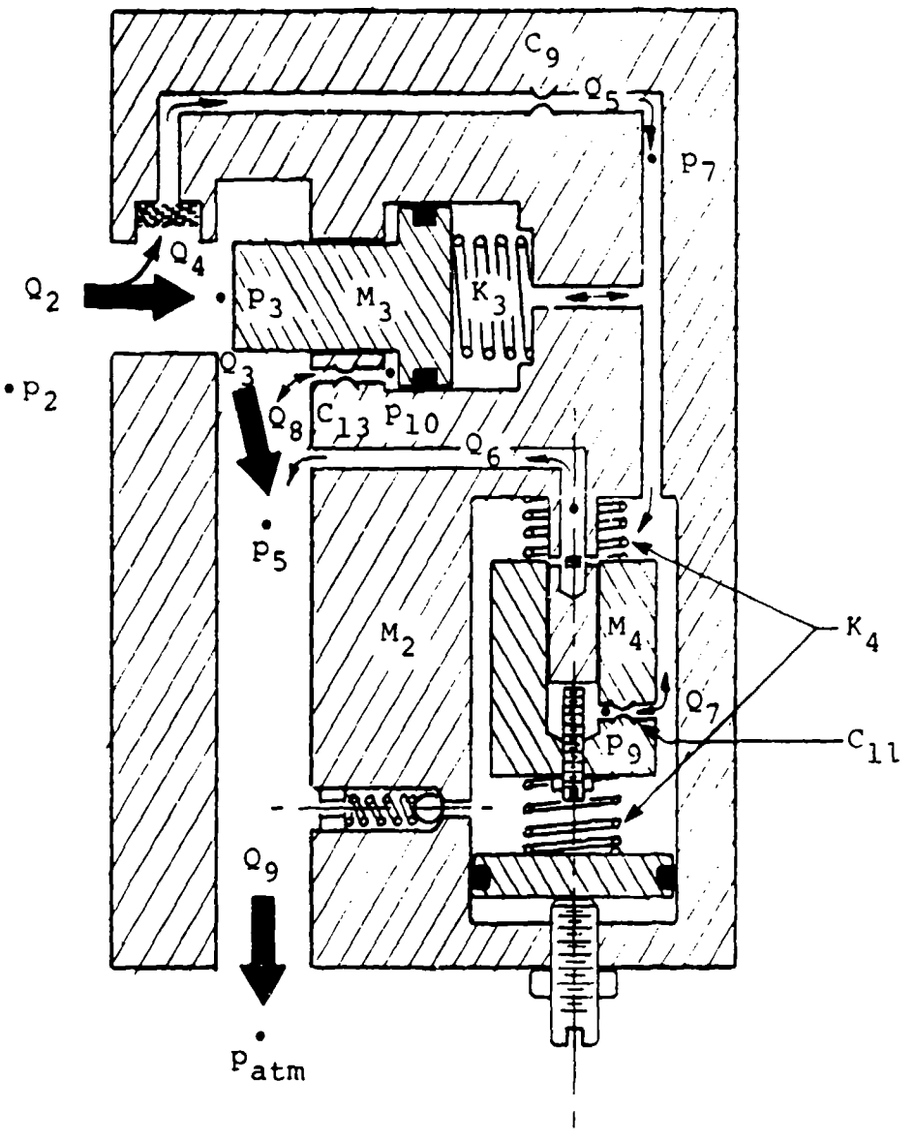

p_i: local fluid pressure

Q_i: fluid flow rate

M_i: segment mass

K_i: spring rate

C_i: orifice coefficient

Figure 4. Schematic diagram of ASAVLEA computer model.

This equation could be rewritten for solution as:

$$P_1 - P_2 - \beta Q_0^2 = 0$$

where $\beta = \rho/2C_0^2A_0^2$ was assumed to be a constant. In order to linearize this type of equation to make it amenable to simple solution techniques, the square root of the pressure drop from the previous time step was used. This equation could then be written in the following form:

$$\frac{P_{1_i} - P_{2_i}}{\sqrt{P_{1_{i-1}} - P_{2_{i-1}}}} - \sqrt{\beta}\, Q_0 = 0$$

Where P_{n_i} is the pressure for the current time step and $P_{n_{i-1}}$ is the pressure from the previous time step. Each of the equations was linearized in this fashion and solved simultaneously when called by the integration subroutine. This recursive technique required the use of a relatively small, fixed integration time step to ensure convergence.

Input to the ASAVLEA computer model consists of: physical dimensions of the valve components (mass, spring rate, and damper values), hydraulic fluid properties, occupant lumped parameters, and a digitized acceleration-time history to use as a driving function. The output from the computer model was intended to aid in interpreting the dynamic performance. At each integration step (or multiple of the time step), all pressures, flow rates, displacements, velocities, and accelerations were printed. Also, a printer-plotting subroutine was incorporated to obtain a pictorial display of the time history of key parameters. These parameters included 1st and 2nd stage pressure, input and occupant acceleration, and displacement of the valve spools relative to the ASAVLEA housing.

The computer model served three functions. It was compared to hand calculations of performance under specific, limited conditions (such as steady state and maximum flow). Then it was used to evaluate dynamic performance under realistic crash conditions. This led to modification of several design parameters in order to optimize dynamic performance. Also, the computer model was used to investigate the sensitivity of performance to various design parameters.

A comparison of the predicted and experimental ASAVLEA performance is discussed in the "Dynamic Testing" section. Appendix A presents a complete printout from one of the simulations.

Discussion of Relief Valve Development

In the evolution from concept to hardware, many decisions had to be made to select the correct combination of masses, springs, and passage sizes. Although many of the decisions used routine control theory and fluid flow principles, a few deserve further explanation. For instance, the orifice identified as orifice 1 in Figure 2 needed to be replaced by the pressure-compensated orifice. This need was related to response speed and unwanted fluid impulse forces which are explained more fully in the following sections.

Response Speed

In the 95th-percentile crash represented by MIL-S-81771 Dynamic Test No. 1 (Reference 1), the seat's energy-absorbing system needs to stroke approximately 10 in. in about 0.110 sec. During this stroke the rate of elongation reaches a peak of about 25 ft/sec. In the hydraulic energy absorber, flow rises from 0 to 75 gal/min and back to 0 gal/min during this period. As the flow rate changes, the 2nd stage valve must be constantly repositioned to provide the correct pressure drop necessary for 14.5 G.

A further complication arises from changes of occupant weight. A very great range of load (approximately 400 to 1900 lb) must be covered by the hydraulic energy absorber. For the low loads required by light occupants, the 2nd stage valve (starting from a closed position) must be moved to a relatively wide-open position to handle peak flow, and then returned to the closed position as the stroke ends. The low operating pressure requires orifice 1 to be fairly large in order to supply enough fluid to the first stage chamber for sufficient speed of response.

For high loads required to decelerate a heavy occupant, the 2nd stage valve should not move very far; it must remain near the closed position to generate high pressures. The high pressures require orifice 1 to be very small to prevent excessive flow into the 1st stage chamber.

Excessive flow into the 1st stage chamber has two consequences: (1) unnecessarily rapid response of the 2nd stage valve, leading to instability, and (2) high impulse forces upon the 1st stage valve as fluid leaves the 1st stage chamber, which causes errors in detecting acceleration.

According to the computer predictions, a suitable compromise using a simple, fixed orifice could not be achieved for both light and heavy occupants. Therefore, a more complex orifice was necessary.

Pressure-Compensated Orifice

One alternative to the simple orifice 1 of Figure 2 was a pressure-compensated orifice, so called because it allows the same amount of fluid to pass, regardless of the pressure differential acting across the orifice. Such devices are readily available as off-the-shelf items from specialty hydraulic equipment suppliers. A second alternative would have been to design a custom orifice which would decrease flow as pressure increased, an optimum condition for the most consistent response and stability over the entire range of occupant weights.

The first alternative, the pressure-compensated orifice, was selected because of its availability and its adequate performance as predicted by the computer model. A constant flow rate of 2 $in.^3$/sec was predicted by the computer model to avoid both sluggish response at low pressures and unstable response at high pressures.

A pressure-compensated orifice providing this flow for the 50 centistoke silicone fluid was purchased from LEE Corporation of Westbrook, Connecticut, for use on the test hardware.

Impulse Error

The 2 $in.^3$/sec flow through the 1st stage chamber exits through the tiny ports of the 1st stage valve at very high velocity, especially when the pressure is high. The forces acting upon the fluid as it converges and accelerates toward the valve ports is felt by the G-sensing mass. The force has been labeled "impulse error" and has been calculated to vary from 0.25 to 0.55 lb (for steady state conditions) depending upon the pressure. This impulse error acts upon the G-sensing mass in a direction opposite to the inertial force of the G-sensing mass. (Recall that the inertial force of the G-sensing mass is proportional to the acceleration to be detected).

If the impulse error were constant, it could be corrected by a readjustment of the first stage preload spring. Only the non-constant portion, 0.3 lb (the difference between 0.55 and 0.25 lb), contributes uncertainty to the detection of acceleration. If the uncertainty is to be limited to 10 percent of the inertial force of the G-sensing mass, then the G-sensing mass must supply 3.0 lb of inertial force at 14.5 G. Therefore, the 1-G weight of the G-sensing mass must be $\frac{3.0}{14.5}$ = 0.2 lb. The size of the G-sensing mass was determined by this method and verified by the computer simulation.

Other Influences on Accuracy

If impulse error were the only error affecting the system, the acceleration of the 95th-percentile occupant would be expected to be 10 percent higher than that of the 5th-percentile occupant. Fortunately, another influence of approximately equal magnitude acts in the opposite direction. This influence is a result of the different equilibrium positions required of the 1st stage valve for different sized occupants. The equilibrium positions, expressed as distance from the fully closed position, are 0.003 in. and 0.0015 in. for the 5th and 95th percentiles, respectively. Because the spring rate of the 1st stage valve is 216 lb/in. the deflection between the two positions requires a force of 0.32 lb. This force acts in the opposite direction of the impulse error and is nearly the same magnitude Therefore the accelerations of the 5th and 95th percer converge to the same value. It is fortunate that this occurs, because the spring rate cannot be adjusted freely over a very wide range to achieve this condition. The choice of the 1st stage spring rate is based primarily upon frequency response requirements revealed by the computer model.

Another factor influencing accuracy is related to disequilibrium, and is best illustrated by Figure 5. The average lumped mass acceleration can be seen to be higher than 14.5 G during the first 0.050 sec and lower during the remaining time. In explanation, fluid flow through the 2nd stage valve is proportional to rate of energy absorber elongation and as the flow increases during the first

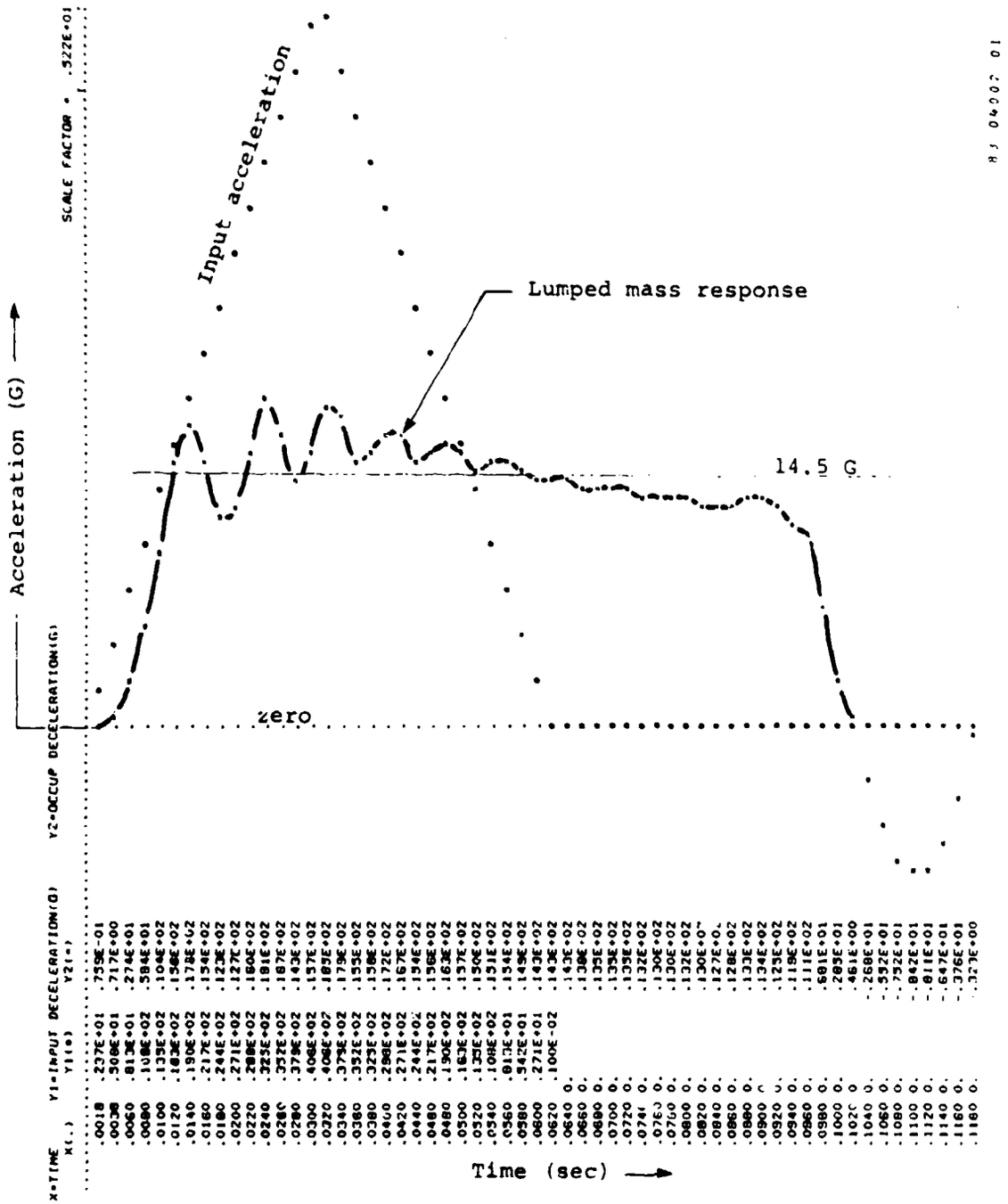

Figure 5. Computer simulation of lumped mass representing the 5th-percentile occupant decelerated by a hydraulic energy absorber. Conditions:

- Occupant effective weight of 112 lb combined with 23-lb bucket.
- Fixed-load energy absorber of 1350 lb used in conjunction with hydraulic energy absorber.
- Spring rates of energy absorbers are representative of actual hardware.

0.050 sec, the 2nd stage valve must gradually open. To cause the 2nd stage valve to open, the 1st stage valve needs to be opened beyond its equilibrium position (i.e., reach disequilibrium), to dump more fluid from the 1st stage than is entering through orifice 1. To hold the 1st stage valve open beyond its equilibrium position requires greater than 14.5 G, which is the disequilibrium error.

After 0.050 sec the 2nd stage valve needs to begin closing as the fluid flow rate decreases, and the reverse of the previous description applies.

If the input acceleration is very brief, such as in the tests described in the "Dynamic Testing" section, the peak flow rate is reached almost immediately. In this case the initial positive disequilibrium error may be very large and brief, or it may be obscured by other transients; the subsequent negative disequilibrium error may be prolonged and small.

Another influence seen in Figure 5 is an oscillation of about 120 Hz in the lumped mass response which damps out slowly. These oscillations result from the underdamped condition of the 1st stage. The underdamped condition was chosen because it provides the quickest response to step inputs, and because the high frequency does not have any detrimental effect upon the human spine. The human body's natural frequencies are much lower, and have the effect of filtering out (averaging) high frequency oscillations. Therefore, the oscillations are not treated as a degradation of accuracy.

Still another influence on accuracy is friction between the G-sensing mass and the tube upon which it slides. Test accelerations in this program were not applied in directions which would have contributed to friction between these parts. In more representative crash conditions, forward and lateral acceleration could be expected to press the G-sensing mass against the tube. Even so, friction forces may be avoided by the hydrodynamic lubrication of fluid leaking between the parts. Alternatively, friction may be overcome by the vibration caused by fluid turbulence. These speculations regarding friction were not investigated by the tests conducted in this program. If future tests indicate that friction is a problem, the G-sensing mass could be supported on a friction-free flexible metal diaphragm.

DESCRIPTION OF TEST ARTICLE

The test hardware incorporates the basic features previously described in sections "Concept Description" and "Development", but packaged in a manner appropriate for repeated testing, readjustment, and maintenance. An extremely rugged design was chosen to endure not only repeated testing, but also extraordinarily high loads which might result from a malfunction.

The ruggedness and special adjustment features resulted in the test hardware being heavier and larger than the alternate configuration described in section "Compact Hydraulic Energy Absorber Size and Shape." That section illustrats that the relief valve can be repackaged inside the piston to produce a compact envelope. Even though the test hardware relief valve is contained in a large housing bolted to the outside of the cylinder, the components within that housing are sized appropriately to be packaged within a piston 1.25 in. in diameter by 3.5 in. long. The results from the hardware test can therefore be applied with confidence to the performance of a production-sized system.

The description of the test hardware is presented in the following tabulations and text, and in the reduced engineering drawings of Appendix B.

Overall Appearance and Size

The outward appearance of the test hardware is shown in Figure 6, with all parts analogous to those previously shown in Figure 1. Overall dimensions and weight are shown on Drawing No. SK 10640 of Appendix B.

Figure 6. Acceleration-sensing automatic variable-load energy absorber.

The hydraulic cylinder used for the energy absorber was a commercial high pressure cylinder manufactured by Norcap, with a 1.5-in. diameter piston, 1.00-in. diameter rod, and 23-in. stroke. Fluid passages in its ends were bored out to avoid restriction, and features were provided for the attachment of the automatic relief valve, P/N 100630.

Details of Automatic Relief Valve

The relationship between the components of the automatic relief valve are shown in assembly Drawing No. SK 10630, and the unique machined components are detailed in Drawings No. SK 10631 through SK 10635. Dimensions, weights, spring

rates, materials, and other pertinent data necessary to reproduce the test hardware may be found on the drawings.

Comparing SK 10630 to Figure 2, most components can be identified by their names and the positions they occupy. The exception is that the filter and orifice which meters fluid to the first stage (items 20 and 19) are shown on SK 10630 located within the second stage spool (item 2) to save space. In this position they serve the same exact function as that shown in Figure 2. In other words, no functional relationship is to be inferred from the concentric relationship between items 2, 19, and 20. Item No. 19 is a pressure-compensated orifice which flows 2 $in.^3$/sec regardless of the pressure differential acting on it.

The fluid used to fill the hydraulic energy absorber was Dow Corning type 510, 50 centistoke, silicone fluid. To avoid trapped air, the hydraulic energy absorber was degassed with a vacuum pump prior to almost every test. (The effect on performance resulting from trapped air is further treated in sections "Development" and "Dynamic Testing.")

The acceleration at which the hydraulic energy absorber will extend is determined by adjusting the acceleration selector screw (item 22 on Drawing No. SK 10630). Prior to the dynamic tests this screw was preadjusted to approximately the correct degree calculated from static tests. The accessibility of the screw permitted convenient readjustment during the test sequence, if such action was found to be necessary.

DYNAMIC TESTING

The primary objective of the testing was to determine if the ASAVLEA could indeed provide constant deceleration for different masses. The test masses were 135 and 223 lb, which represented the total effective weights of the 5th- and 95th-percentile occupants in a seat bucket weighing 23 lb. The following is a description of the test apparatus, instrumentation, test conditions and results.

Test Apparatus

The test apparatus can best be understood by comparing the pretest and posttest photographs of Figure 7 and studying the following description. The test apparatus consists of the major components listed below:

- Test mass assembly
- Hydraulic energy absorber
- Fixed-load energy absorber
- Drop cage
- Tower

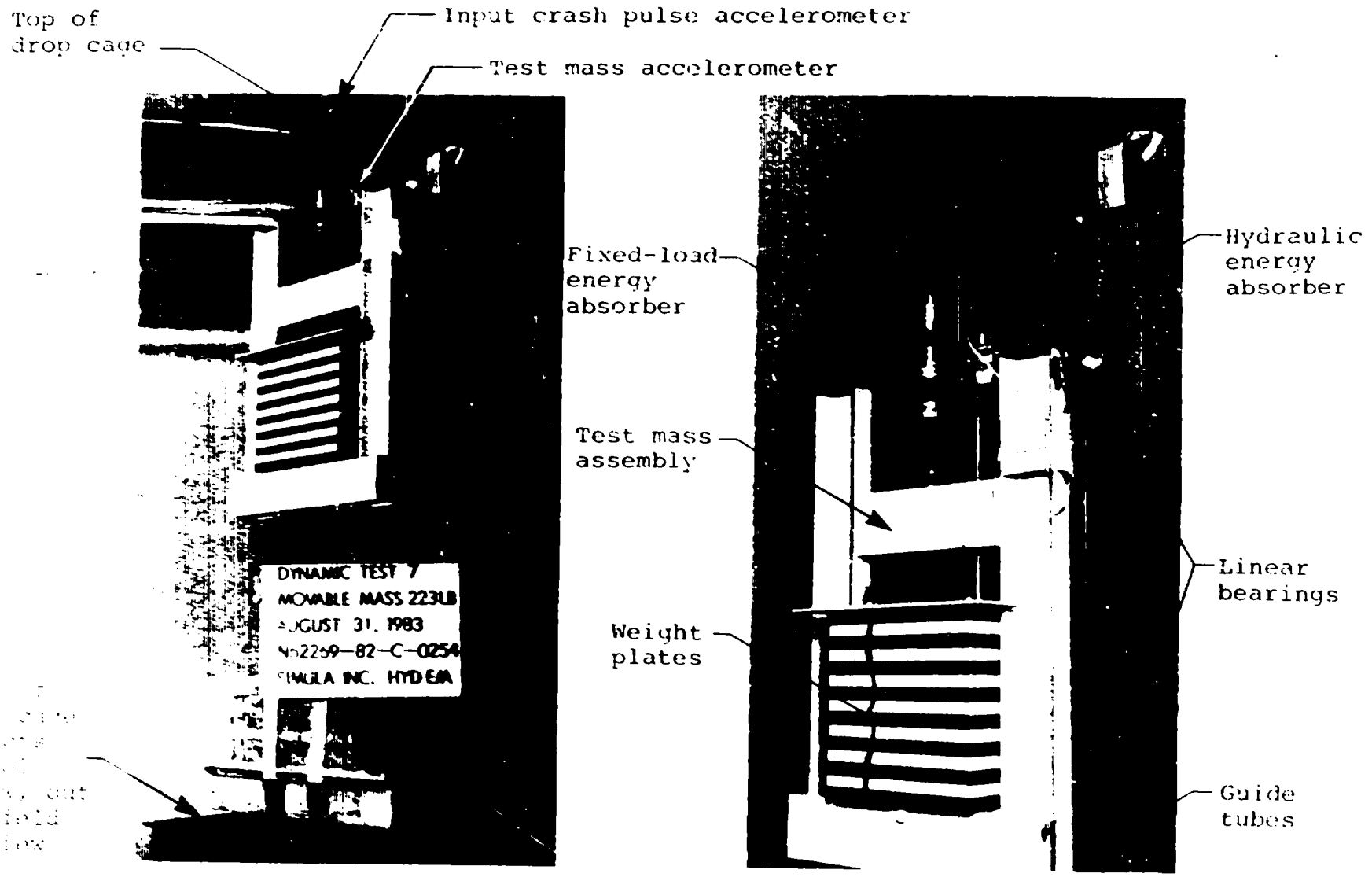

a. Pretest test setup.

b. Posttest view showing stroked energy absorbers.

Figure 7. Test apparatus.

- Gravel pile impact barrier
- Accelerometers and instrumentation.

The test mass was guided in the intended direction of its motion by linear bearings and guides between it and the drop cage. The total weight of the test mass included the test mass frame, weight plates bolted to it, guiding linear bearings, and attached energy absorbers. The weight of the test mass was adjusted by changing the quantity of weight plates.

The test mass was supported in the direction of the inertial loads by the hydraulic energy absorber (Drawing No. SK 10640) and by a fixed-load inversion tube energy absorber (Simula P/N 100566). The inversion tube provided a dynamic load of approximately 1350 lb, and the hydraulic energy absorber was required to provide whatever additional load was required to decelerate the test mass at 14.5 G.

Test Procedure

To prepare for a test, the drop cage was raised on the tower and the gravel pile beneath it was stacked to a predetermined height and shape. Then, to perform a test, the cage was driven downward to impact the gravel pile. A nitrogen charged accumulator, valve, and cylinder mounted on the back of the tower (not shown in Figure 7) were used to accelerate the cage downward. The impact of the cage with the gravel pile was sensed by an accelerometer and identified as the "input crash pulse." Acceleration of the test mass assembly was sensed by a second accelerometer and recorded as the "test mass acceleration."

The accelerometer outputs were amplified and filtered at 300 Hz with signal conditioners and immediately fed to and captured by a digital waveform analysis system (Norland 3001). Timing for the Norland's data sampling was set at 1 msec per data point, and the capture period was initiated by triggering the analysis system via a micro switch located at the accumulator control valve. The captured data were then stored on computer disks for analysis and plotting.

Prior to transfer to the x-y plotter, the data were further conditioned using the Norland's "10 N point average" capability, which uses a weighted, moving average of 10 points in the data array, thus providing a slight smoothing effect.

The instrumentation used for these tests are presented in Table 2.

Test Conditions and Results

At first, the magnitude and duration of the input crash pulse was built up gradually to selectively investigate the performance of the ASAVLEA and the test apparatus. When the crash energy was raised to a sufficient magnitude, the energy absorbers were required to stroke, but the stroking distance was very short (between 2 and 6 in.). Results of these low-energy tests are presented in Figures 8 through 11.

As the input pulse was further increased, a limitation of the test fixture was discovered which prevented simultaneous control of the onset rate and peak acceleration of the input crash pulse. Fortunately, the hydraulic energy

TABLE 2. TEST INSTRUMENTATION

Item	Instrument	Type	Manufacturer	Model	Range	Response	Accuracy full-scale (percent)
1	Accelerometer	Unbonded Strain Gage	Bell & Howell	4-202	100 G	1250 Hz	0.75
2	Signal Conditioner	Bridge Offset	Bell & Howell	1-183	± 1V	DC to 30 KHz	0.1
3	Digital Voltmeter	Digital	Valhalla	4440	± 2V	N/A	0.05
4	Waveform Analyzer System	Digital	Norland	3001	± 100 m.v to 100 V	Flat within 0.5 percent DC to 60 KHz	0.75
5	X-Y Plotter	Potentiometric	Plotamatic	715	1 mv/in. to 10 V/in.	N/A	0.2

absorber appeared to be tolerant to onset rates higher than the 2,100 G/sec expected in realistic crash situations. Therefore, testing was continued even though the severity of the input crash pulse exceeded the target values. Figures 12 through 15 reveal the performance of the hydraulic energy absorbers when subjected to the most severe input pulses that the test fixture could deliver. Table 3 summarizes the conditions and results, including measured displacements and velocities calculated from the acceleration data.

The only times during the test series that the acceleration selector screw of the hydraulic energy absorber was adjusted, was after Tests 3 and 5, as shown in Table 3. This is important when tests such as 6 and 7 are compared to each other: these test masses were different, and the constant value of the acceleration plateau can be attributed solely to the automatic action of the hydraulic energy absorber.

Interpretation of Results

In general, the hydraulic energy absorber demonstrates the desired performance by limiting the test mass acceleration to a predetermined value regardless of the size of the mass. Tests 1 through 4 illustrate the hydraulic energy absorber's ability to respond without overshoot to a realistic crash acceleration onset rate for test masses of the 5th- through the 95th-percentile. Tests 6, 7, and 8 illustrate that the hydraulic energy absorber can maintain the correct acceleration of the 5th- through 95th-percentile test masses through a sustained stroke during which the elongation velocity reaches 18 ft/sec. Measured accuracy and frequency response also confirm the computer predictions, giving validity to the analytical model.

Two departures from desired performance which require explanation can be seen in Tests 2 and 6. Conditions were nearly identical in Tests 2 and 3 except that the hydraulic energy absorber was vacuum degassed prior to Test 3, but not prior to Test 2. It is believed that air was present in the 1st stage chamber during Test 2, which would result in premature opening of the 2nd stage valve as pressure built, collapsing the air pocket.

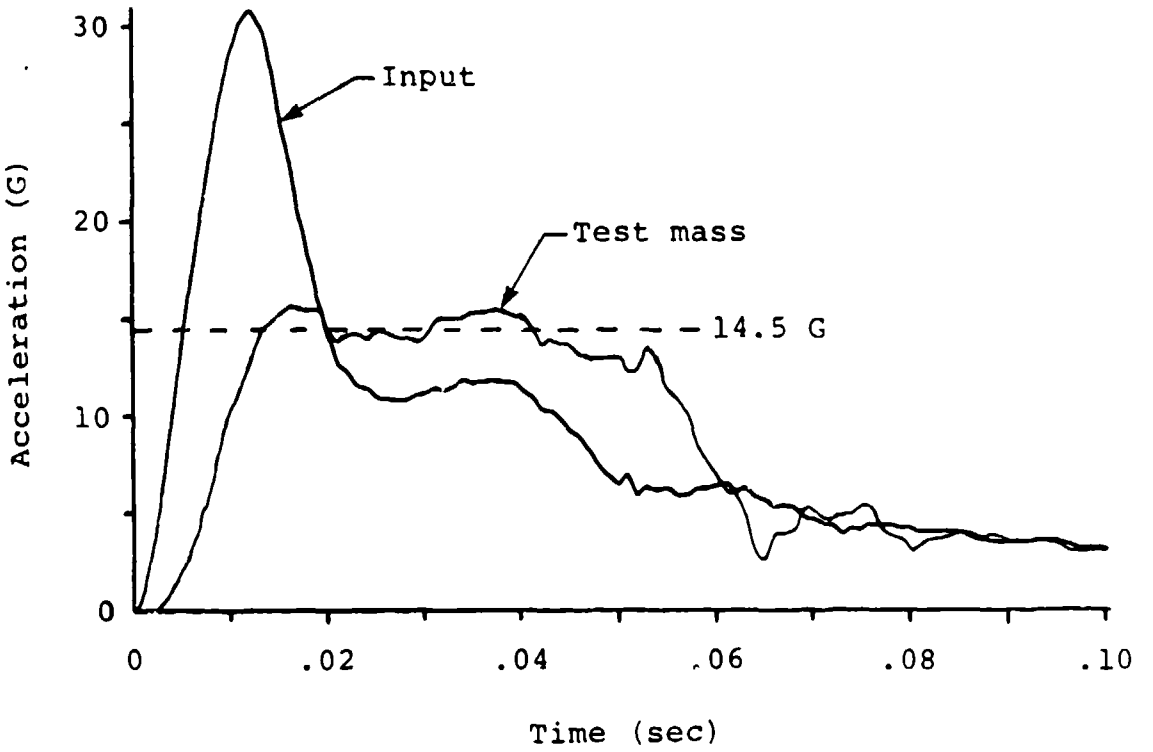

Figure 8. Test 1 with 5th-percentile test mass.

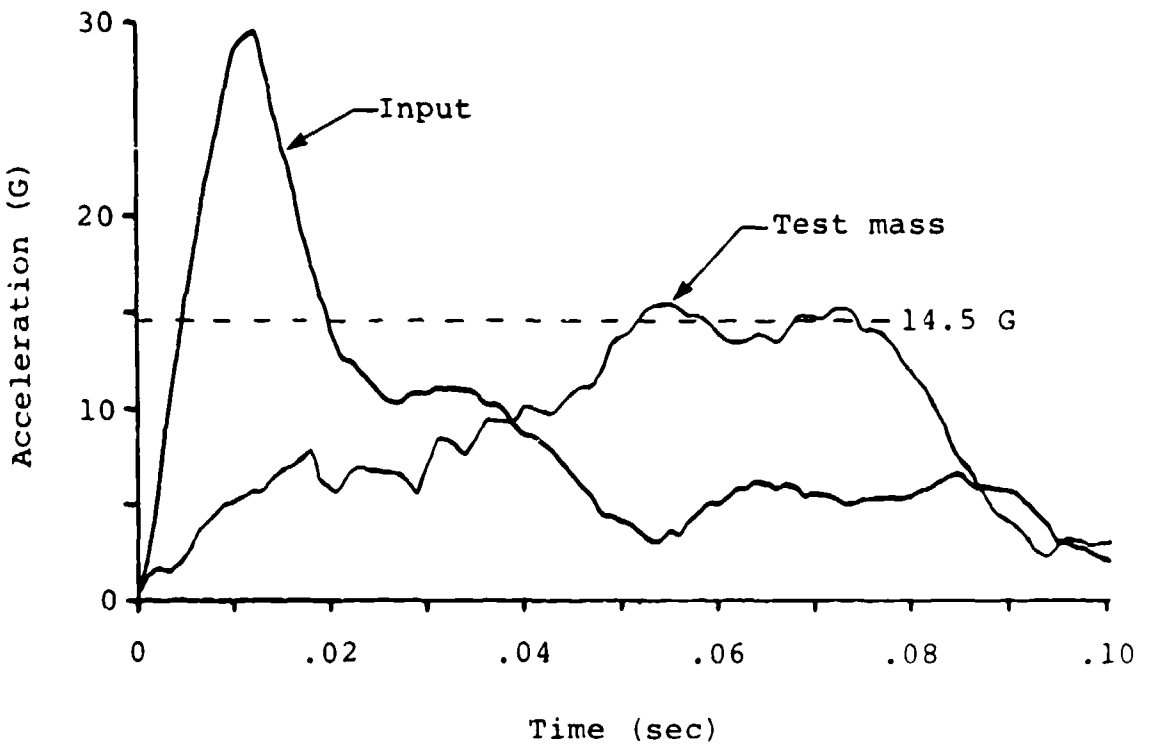

Figure 9. Test 2 with 95th-percentile test mass.

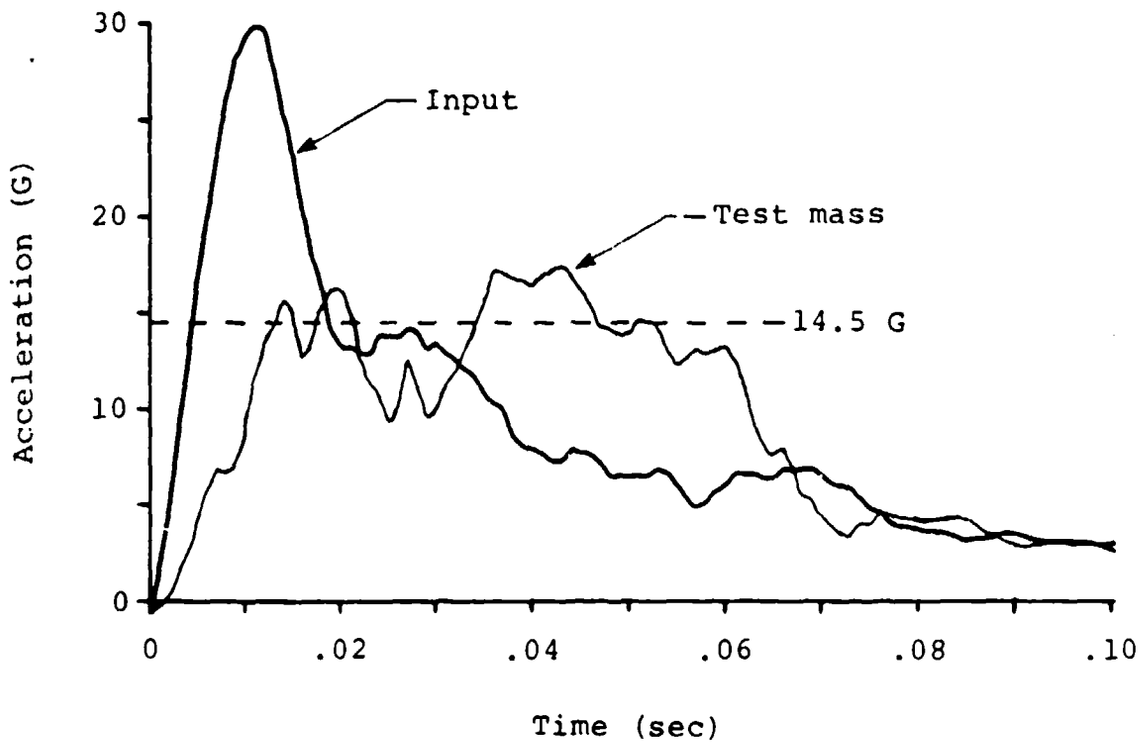

Figure 10. Test 3 with 95th-percentile test mass.

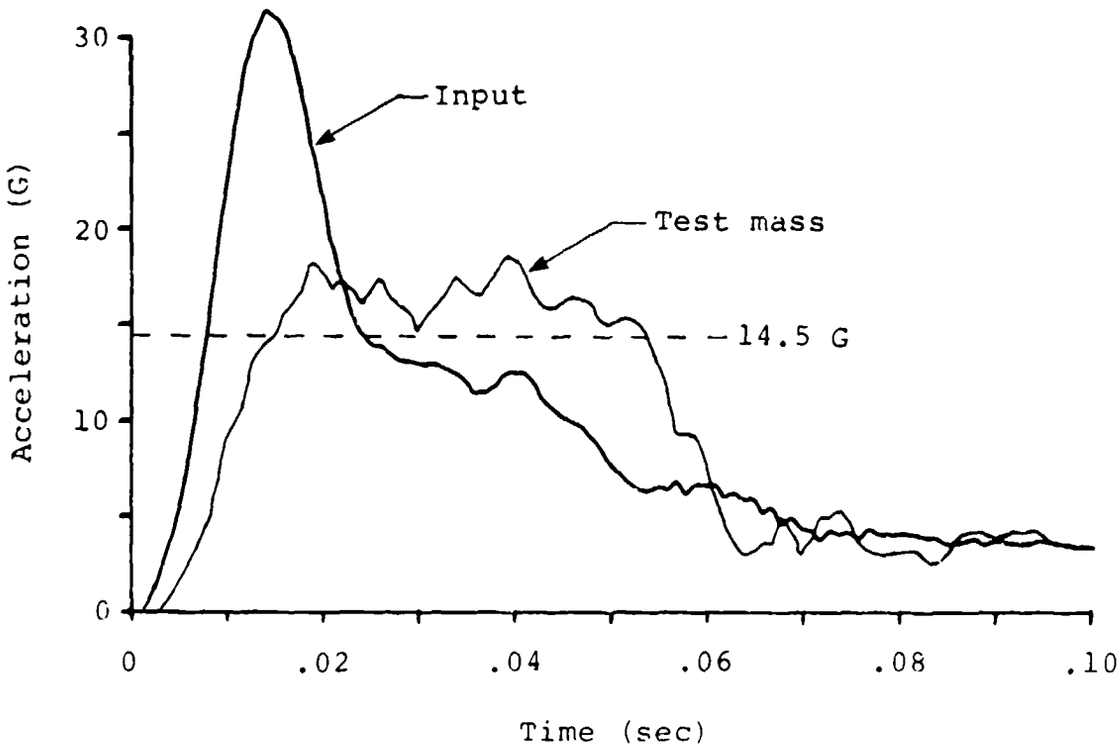

Figure 11. Test 4 with 5th-percentile test mass.

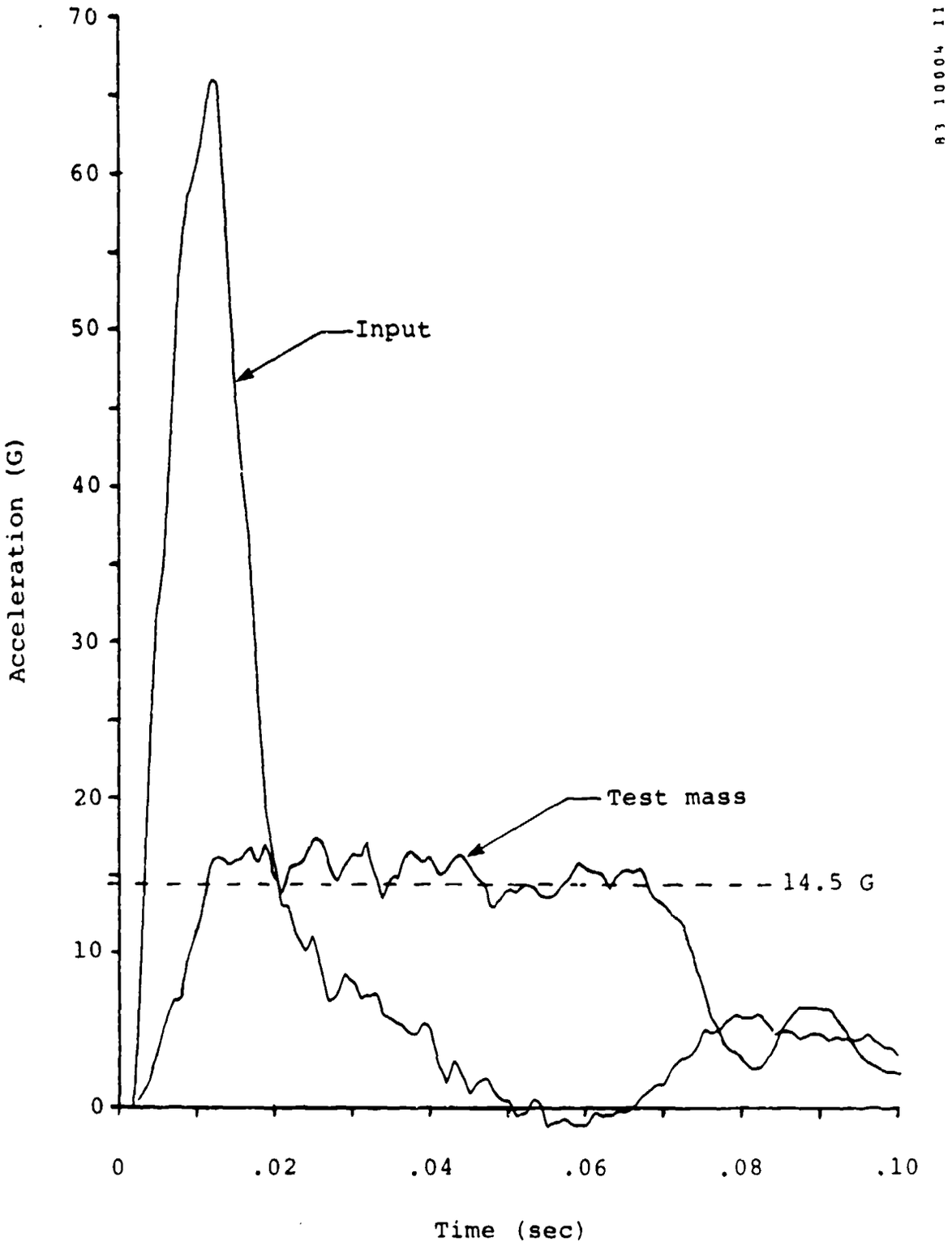

Figure 12. Test 5 with 5th-percentile test mass.

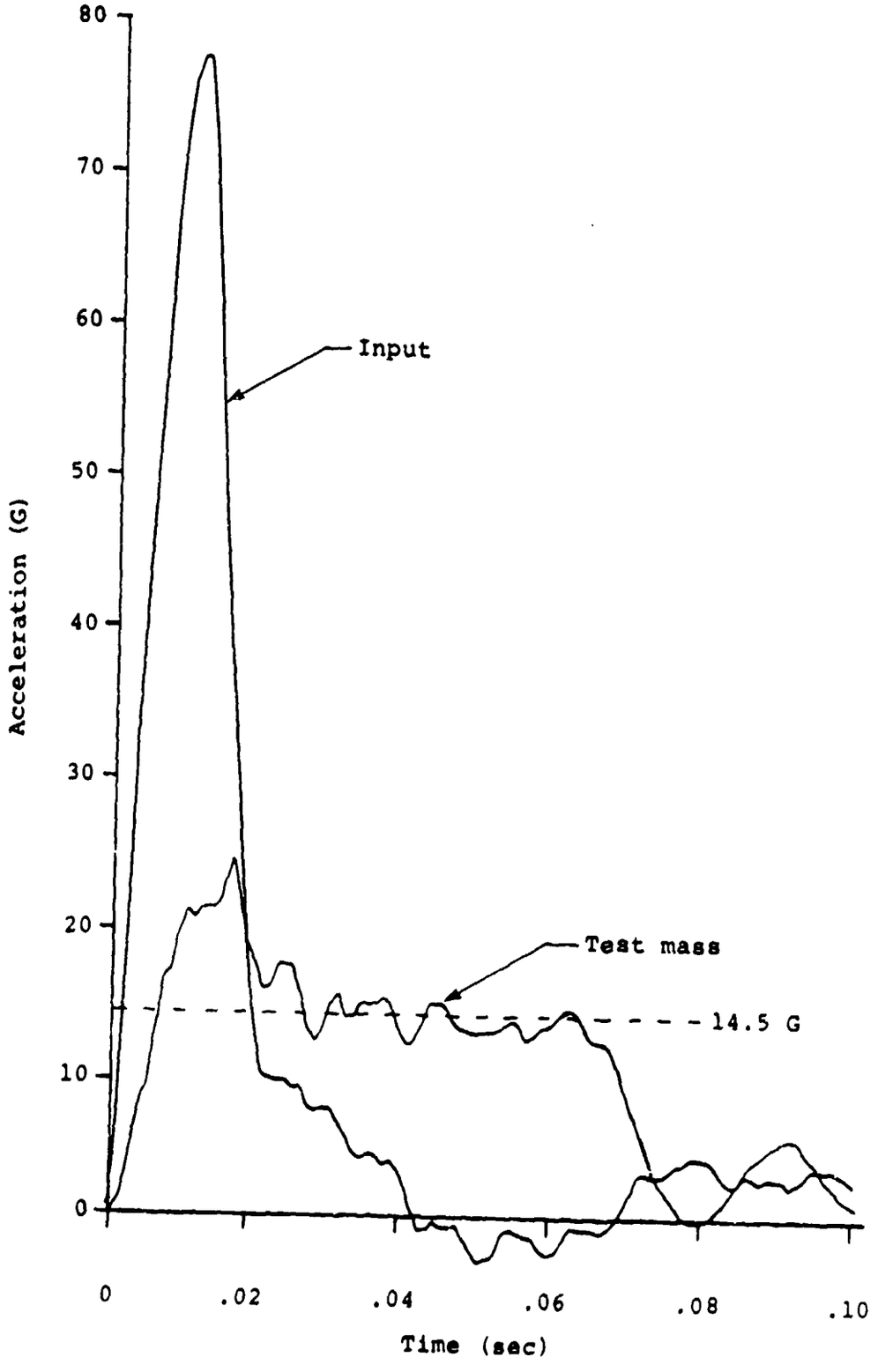

Figure 13. Test 6 with 5th-percentile test mass.

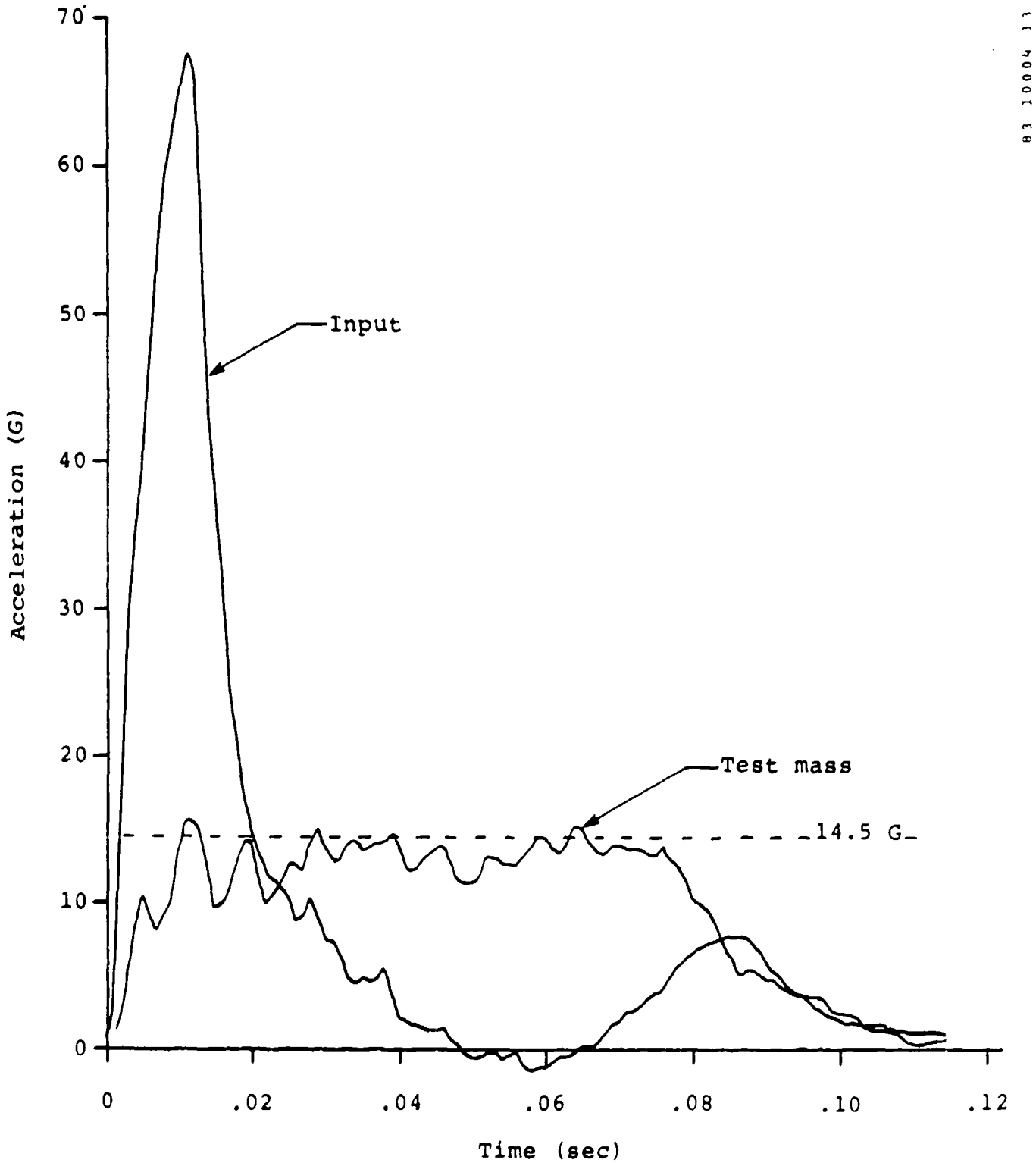

Figure 14. Test 7 with 95th-percentile test mass.

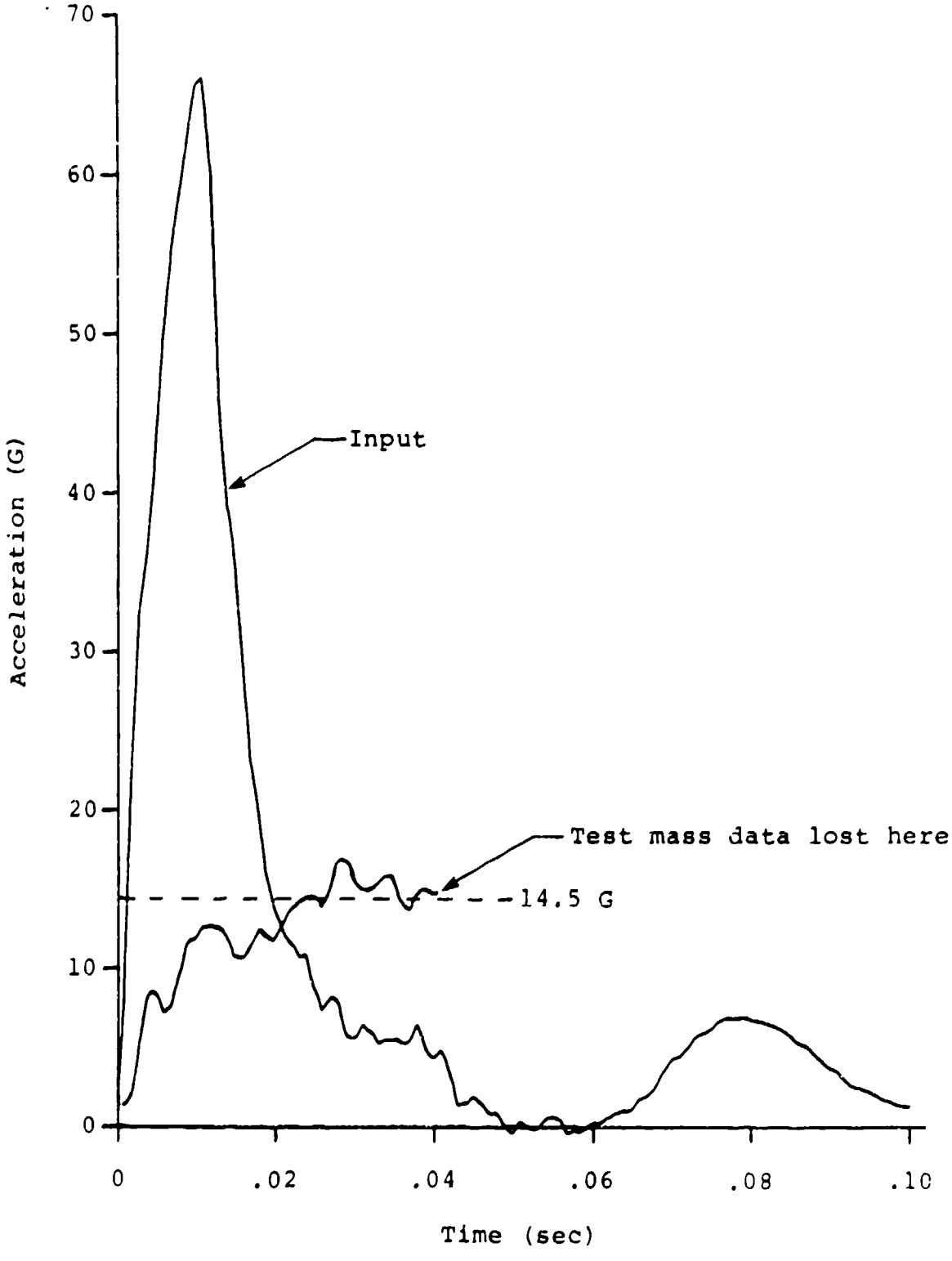

Figure 15. Test 8 with 95th-percentile test mass.

TABLE 3. SUMMARY OF DYNAMIC TEST RESULTS

Test No.	Test Mass (percentile)	Input Crash Pulse: Onset Rate (G/sec)	Input Crash Pulse: Peak (G)	Input Crash Pulse: Velocity Change (ft/sec)	Hydraulic E/A Performance: Average Plateau (G)	Hydraulic E/A Performance: Measured Stroke (in.)	Hydraulic E/A Performance: Maximum Elongation Rate (ft/sec)	Remarks(1)
1	5th	3,100	31	32.0	14.5	2.0	6.7	
2	95th	3,100	29	30.0	14.5	6.2	10.5	(2)
3	95th	3,200	30	32.4	N/A	3.0	6.5	(3)
4	5th	3,100	31	33.0	16.5	2.0	5.7	
5	5th	8,000	66	35.0	15.0	9.0	18.0	(2) (4)
6	5th	8,800	78	35.0	14.0	8.1	18.0	
7	95th	7,400	67	35.0	13.5	9.9	18.0	
8	95th	7,100	66	35.0	N/A	9.2	N/A	

Notes:

1 The hydraulic energy absorber was vacuum degassed prior to each test except as noted.

2. Hydraulic energy absorbers not degassed prior to test. Air bubbles suspected to be present in 1st stage.

3. After this test, the acceleration selector screw was turned 9 degrees clockwise in an attempt to increase the average by 1 G.

4. After this test, the acceleration selector screw was turned 9 degrees counterclockwise in an attempt to decrease the average by 1 G.

At 20 msec into Test 2, the observed acceleration value of 6.5 G was consistent with that which would occur if the fixed-load energy absorber acted alone ($\frac{1350}{223} = 6$). The hydraulic energy absorber was not yet contributing any significant load. By 55 msec, the air apparently was purged or compressed to a small enough volume to be negligible, at which time the hydraulic energy absorber began to function correctly.

In Test 6, the test mass acceleration overshot the plateau value for 20 msec because the extremely high crash pulse onset rate very abruptly caused a high elongation rate of the hydraulic energy absorber. The high elongation rate caused high fluid flow which requires a large opening of the 2nd stage valve to keep the force down to that required by the 5th-percentile test mass. The second stage valve, which always starts closed, was simply unable to open fast enough.

Compare the conditions of Test 6 to those of Test 5. In both cases input acceleration onset rate is excessive, approximately 8,000 G/sec. The hydraulic energy absorber was not degassed prior to Test 5 and the probable presence of air in the first stage chamber may have permitted the 2nd stage valve to open more rapidly. Although the test mass acceleration of Test 5 has the desired shape, it is probably the result of two offsetting undesired conditions: excessive crash input onset rate combined with a small amount of trapped air.

In Test 7, the 95th-percentile test mass requires very high loads from the hydraulic energy absorber. This, in turn, means that the 2nd stage valve does not have to open as far. It appears that, even in spite of the excessive

onset rate of the input crash pulse, the hydraulic energy absorber was able to keep pace.

Test 8 was a rerun of Test 7 to examine the repeatability of the ASAVLEA. In both Tests 7 and 8, the hydraulic energy absorber was degassed and subjected to the same crash conditions. The similarity of results in Tests 7 and 8 over the first 20 msec indicate no significant difference in the amount of gas present. It is unlikely that gas existed after the degassing procedure, especially in repeated tests having the same results. In Test 8 at 40 msec, data was lost when an accelerometer cable was broken by the stroking test fixture. Nevertheless, the performance after 40 msec in Test 8 can be inferred to be similar to that of Test 7 due to the similar total measured stroke, thus demonstrating repeatability.

Vacuum degassing of the hydraulic energy absorber was performed prior to every test except 2 and 5; only in Tests 2 and 5 did results indicate the presence of gas. The entry of gas into the hydraulic energy absorber between tests was inevitable due to inability of the cup seal on the cylinder rod to stop the entry of air. The cup seal is oriented to block internal pressure, not vacuum. This is a shortcoming of the test hardware which could be eliminated on future revisions of the hydraulic energy absorber if an O-ring were substituted for the cup seal. The O-ring would block leakage in both directions.

ALTERNATE CONFIGURATION

The test hardware described in the section "Description of Test Article" was made especially rugged and heavy for repeated testing. Although its dynamic performance can be compared directly to other energy-absorbing systems, its weight and size cannot. Therefore, the following text and illustrations are presented to describe a more compact, lightweight version of the hydraulic energy absorber. Also introduced in the following discussion is a feature necessary to compensate for temperature expansion of the fluid.

Compact Hydraulic Energy Absorber Size and Shape

The length and diameter of the hydraulic energy absorber depends upon the stroke and force required. As in previous examples within this report, the requirements of the SH-60B Seahawk seat were chosen, allowing direct comparison to be made to the mechanical, manually adjustable system described in Reference 4.

The overall size and weight of the alternate lightweight hydraulic energy absorber are shown in Figure 16 and Table 4. The piston/relief valve and the temperature compensating bladder are discussed more fully in the following sections.

Piston/Relief Valve

As mentioned in "Description of Test Article," the components of the relief valve were sized with the intention of packaging them within a piston 1.25 in. in diameter, even though they were packaged in the sizable external housing for testing. The recommended repackaging of those components within the piston is shown in Figure 17.

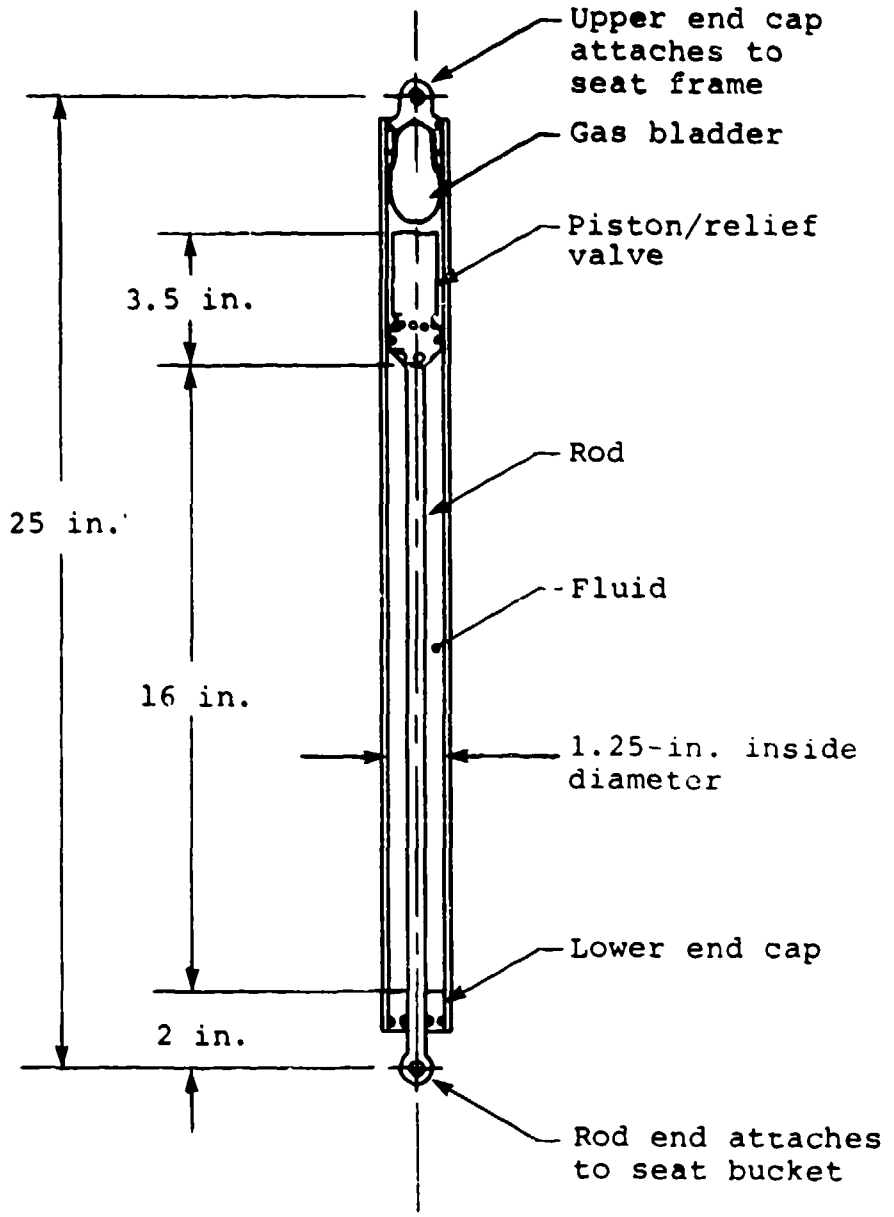

Figure 16. Compact hydraulic energy absorber configuration.

Temperature Expansion Compensation

Over the required operating range of -60°F to +160°F, the volume of the silicone oil (or of most other hydraulic fluids) can be expected to change by almost 10 percent. The gas-filled bladder above the piston can permit this to occur safely. The gas must be kept out of the relief valve by containment in the bladder, and the bladder must be located on the low pressure (top) side of the piston to prevent "sponginess" in the high pressure side of the piston. Although the bladder is on the opposite side of the piston containing most of the fluid, the fluid will be able to slowly leak through the 1st and 2nd stage valves even though the valves are normally closed. Because of such fluid

TABLE 4. WEIGHT SUMMARY, COMPACT HYDRAULIC ENERGY ABSORBER

Component	Material	Weight (lb)
Cylinder	Aluminum tube	.5
Rod	Steel tube	.5
End Cap, Upper	Aluminum	.1
End Cap, Lower	Aluminum	.1
Piston/Relief Valve	Stainless Steel	.8
Fluid	Silicone	.6
Total		2.6

leakage in either direction through the 1st stage chamber, a filter on the outlet, as well as on the inlet, of the 1st stage chamber is required.

COMPARISON OF ASAVLEA TO MAVLEA

The acceleration-sensing automatic variable-load energy absorber (ASAVLEA) has been shown in the section "Dynamic Testing" to perform well when required to provide constant deceleration to different lumped masses, and to require no need for adjustment. This is a definite advantage over a manually adjusted variable-load energy absorber (MAVLEA), which requires adjustment, and therefore is subject to possible maladjustment. It has an even greater advantage over fixed-load energy absorbers which cannot be optimized to the mass.

In addition to ease of use and performance when decelerating a lumped mass, other factors need to be considered to complete the comparison: performance when decelerating a distributed mass system, size and weight, reliability, accuracy, maintainability, and cost. The following discussion compares the ASAVLEA to the MAVLEA on all the above factors. Performance with lumped masses is based upon the actual tests described in "Dynamic Testing," and performance with distributed masses is based upon computer predictions using occupant and bucket stiffness and mass distributions according to the best available information. Other factors are evaluated using the compact alternate configuration shown in the section "Alternate Configurations."

Dynamic Performance

Dynamic performance of the ASAVLEA has been predicted for the deceleration of both lumped and distributed masses, and actually measured for the lumped mass case.

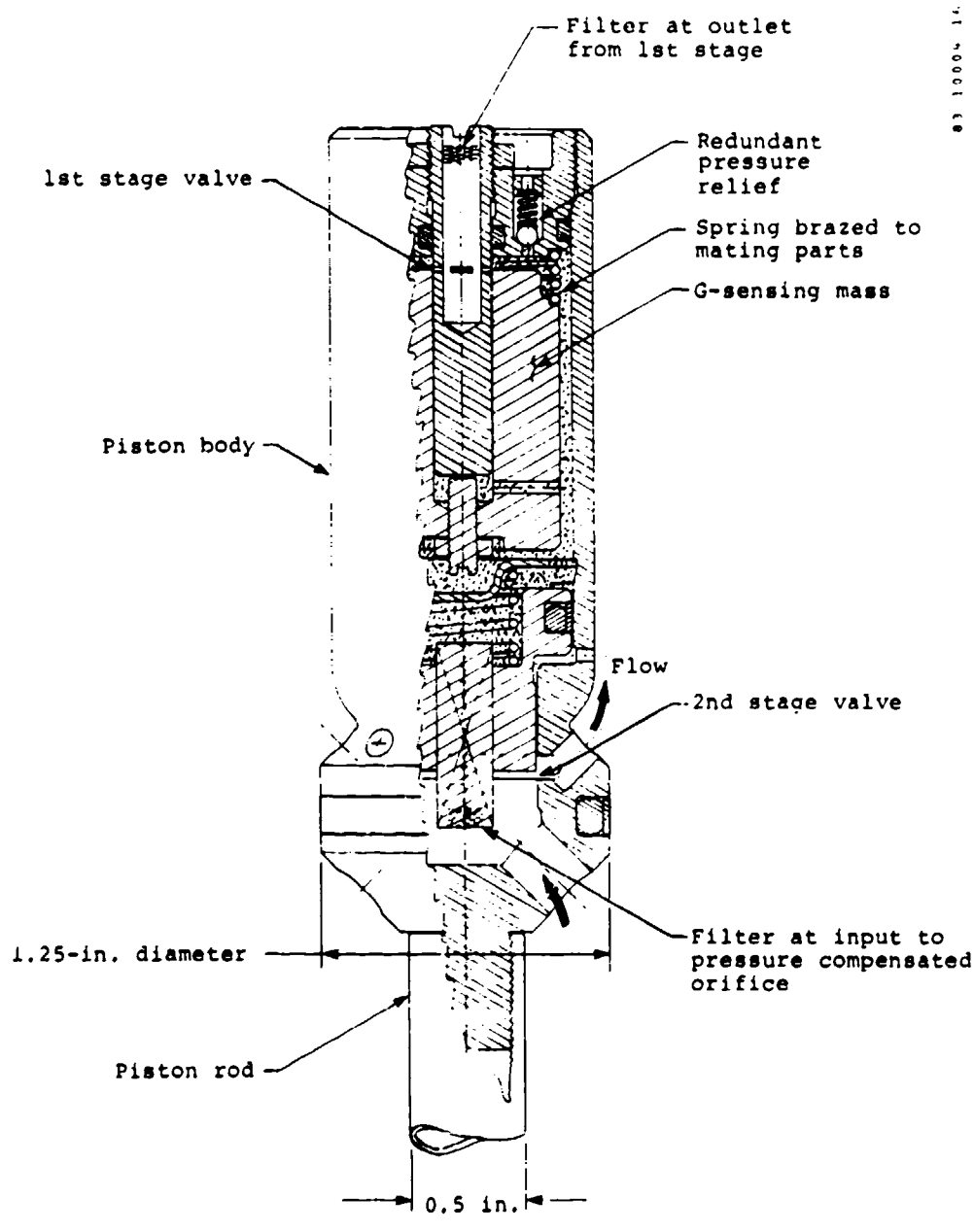

Figure 17. Automatic relief valve packaged within piston.

Lumped Mass Case

Agreement between the predicted and measured performance with the lumped mass was good, with the measured acceleration response close to 14.5 G and showing less instability than predicted. Figure 18 is a typical prediction for the lumped mass case, and shows a sustained and growing instability not present in Test 7 (Figure 14).

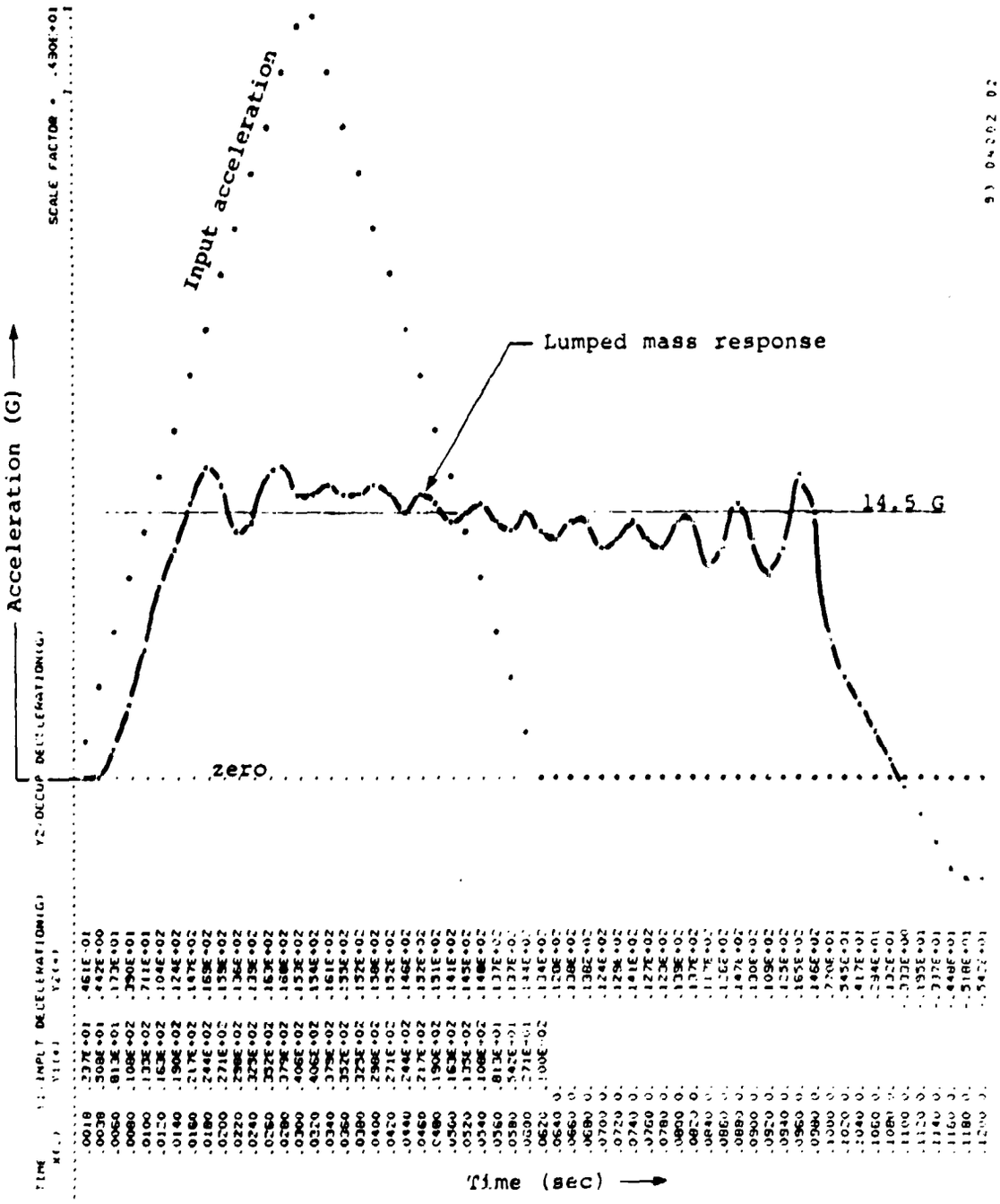

Figure 18. Computer simulation of lumped mass representing the 95th-percentile occupant decelerated by a hydraulic energy absorber. Conditions:

- Occupant effective weight of 200 lb combined with 23-lb bucket.
- Fixed-load energy absorber of 1350 lb used in conjunction with hydraulic energy absorber.
- Spring rates of energy absorbers are representative of actual hardware.

Distributed Mass Case

For the distributed mass case, two different computer representations of the seat/occupant energy absorber were used: one employed Program SOM-LA (Seat Occupant Model - Light Aircraft) and the other, Program SEAT. The two representations predict different results, but this is not surprising because not only do the SOM-LA and SEAT occupant models vary from one another, but the energy absorber conditions are also different.

The cases with Program SOM-LA were run early in the development series, before the computer model of the relief valve was complete. The acceleration-sensing energy absorber was omitted and its action was simulated by a constant acceleration input to the seat bucket. In contrast, the cases presented in this report which feature Program SEAT use the computer model of the ASAVLEA and a more flexible model of the seat bucket.

Predictions of the computer representation using SOM-LA are summarized in Table 5, and examples of the computer output from which Table 5 was obtained are shown in Figures 19 through 22. Predicted response displayed no instability. Predictions using Program SEAT, shown in Figures 23 through 25, suggest instability within the spring mass system being controlled by the ASAVLEA.

Tentative conclusions can be drawn from these predictions, but first it is important to recognize the following conditions:

1) Neither SOM-LA nor SEAT is entirely accurate in representing response of the seat-occupant system, and neither has been validated under the peculiar conditions for which they were used.

2) Under lumped mass conditions the ASAVLEA was predicted to be more unstable than actual testing confirmed.

3) Other than the weight and overall spring rate, properties of the seat buckets were not precisely known; damping coefficients and mass-spring distributions were estimated using simplifying assumptions and meager data.

Keeping the above limitations in mind, the ASAVLEA's control of a distributed mass system can be expected to experience some instability. Support for this statement comes from interpretations of the data which suggest that the acceleration sensed by the ASAVLEA is predominantly that of a small portion of the seat bucket. Fluctuating forces feeding into this small (mass) portion of the bucket from the larger mass-spring occupant system and from the hydraulic energy absorber itself can cause abrupt acceleration changes which the ASAVLEA cannot correct promptly. If the attempted ASAVLEA correction occurs out-of-phase with the fluctuations of the seat bucket, then the fluctuations will be built higher rather than diminished by the ASAVLEA.

The resonance just described may or may not occur in a real test. Even if it does occur, the frequency is high enough to have little effect on the Dynamic Response Index (DRI). However, as suggested by Figure 24, the resonance amplitude may become so great that the ASAVLEA will fail to converge to 14.5-G average acceleration.

TABLE 5. COMPARISON OF OCCUPANT RESPONSE TO CONSTANT LOAD VERSUS CONSTANT ACCELERATION

Case Code	Seat Bucket and Spring Rate (1)	Total Weight Occupant Plus Equipment (lb)	Type of Energy Absorber (2) Constant Load MAVLEA	Type of Energy Absorber Automatic Set to 14.5 G	Results Predicted by SOM-LA Peak Lumbar Compression Load (lb)	Peak DRI	Results Predicted by SOM-LA Maximum Seat Bucket Displacement (in.) (3)	Results Predicted by SOM-LA Maximum Energy Absorber Load (lb)	Remarks
S5F	23-lb bucket with	136.5	X		1628	18.0	32.2	1937	
S5A	4308 lb/in. spring rate similar to	(lightweight)		X	1627	22.9	32.2	3037	
S3F	SH-60B Seahawk	250.0	X		3224	18.2	34.9	2973	
S3A		(heavyweight)		X	3231	21.7	32.9	5728	
S7F	110-lb bucket with	136.5	X		1844	21.1	32.6	3169	
S7A	4308-lb/in. spring rate similar to	(lightweight)		X	1827	22.7	32.3	5037	
S6F	crewseat of AH-64A	250.0	X		3771	21.9	33.3	4196	
S6A	Apache	(heavyweight)		X	3201	21.2	33.3	7766	
S1F	60-lb bucket	164.0	X		1937	19.5	30.8	2749	15,000 lb/in.
S1A	with spring rate as noted	(medium)		X	2005	-	31.8	-	Rigid seat
S2F			X		2067	20.2	32.0	2753	4308 lb/in.
S2A				X	1896	23.4	32.5	4578	4308 lb/in.

Notes:

1. All cushion properties are the same as those of the UH-60A Black Hawk unless otherwise noted.
2. Constant load which could be provided by a correctly adjusted manually adjustable variable-load energy absorber (MAVLEA).
3. Displacement of bucket relative to the ground; includes deformation of airframe, energy absorber, and bucket.

Dynamic testing of the ASAVLEA with a real seat bucket and anthropomorphic dummy will be needed to answer questions posed by the distributed mass condition. Such activity was outside the scope of this program and beyond the capabilities of the test fixture.

Size and Weight Comparison

Compared to a manually adjustable system, the hydraulic energy-absorbing system is at a disadvantage relative to size and weight, as is indicated in Table 6. The length of the hydraulic energy absorber is a particular disadvantage in retrofit situations. However, for future seat designs, the length could be accommodated, as it is less than the total height of the seat bucket.

Reliability Comparison

Reliability of an energy-absorbing system may be defined in terms of two characteristics: 1) ability to perform without failure, and 2) ability to limit the severity of failures, should failures occur. Both characteristics must be evaluated in both operational and crash conditions.

The reliability of ASAVLEA and MAVLEA systems cannot accurately be compared due to lack of data. However, general features of the hydraulic energy absorber can be treated on an absolute basis; with normal precautions, no great distrust of its reliability is warranted.

In the ASAVLEA system, the hydraulic energy absorber is teamed with a companion fixed-load energy absorber, and the combination improves reliability in both operational and crash conditions. In operational use (normal flight) the 1-G weight of the occupied seat bucket and any downward or upward flight loads up to about 6 G, would be supported not by the hydraulic energy absorber, but by the fixed-load companion energy absorber, the reliability of which is very high.

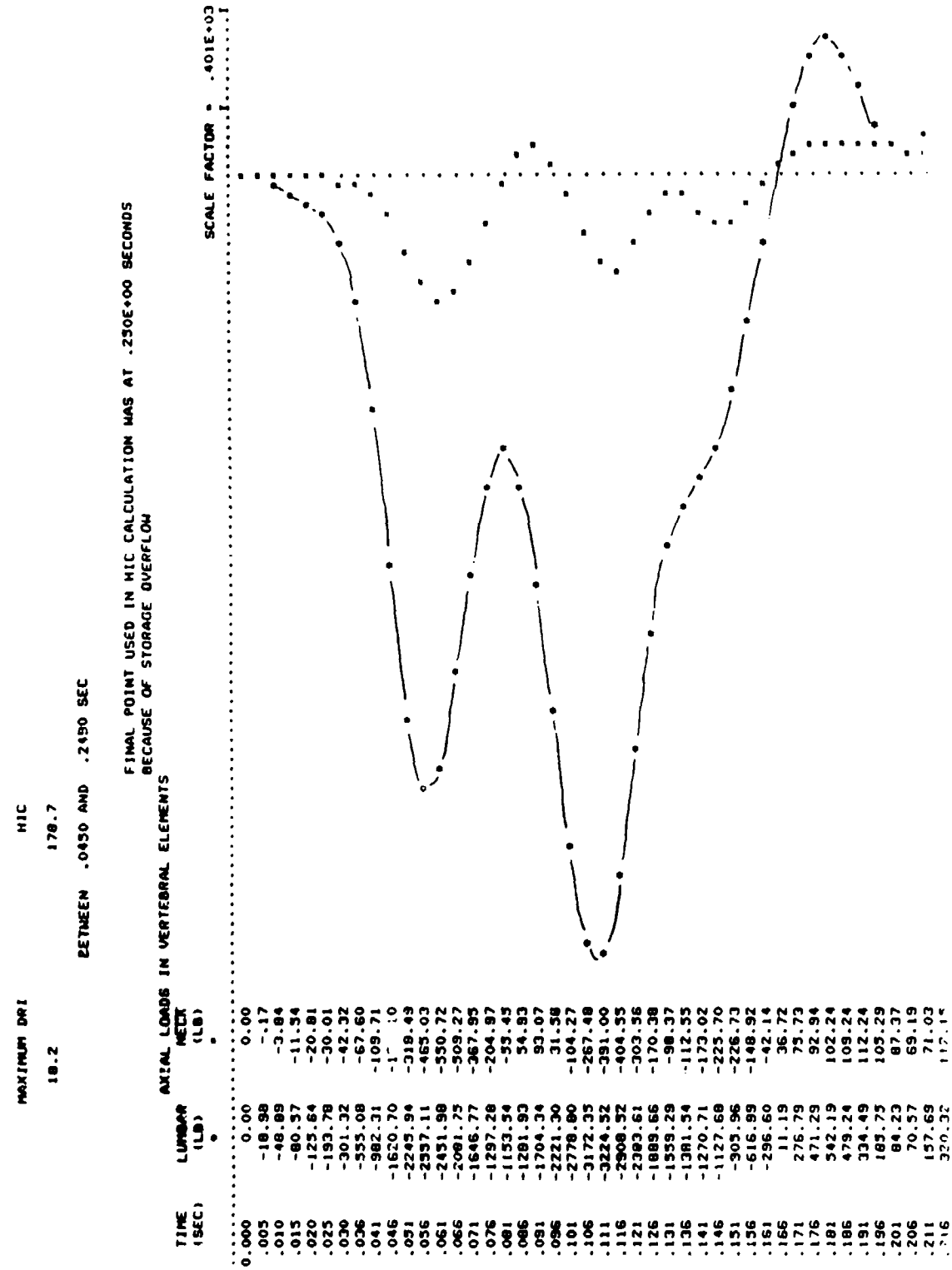

Figure 19. Case S3F simulation of lumbar loads. Conditions: constant force energy absorbers acting on SH-60B Seahawk bucket with heavy occupant.

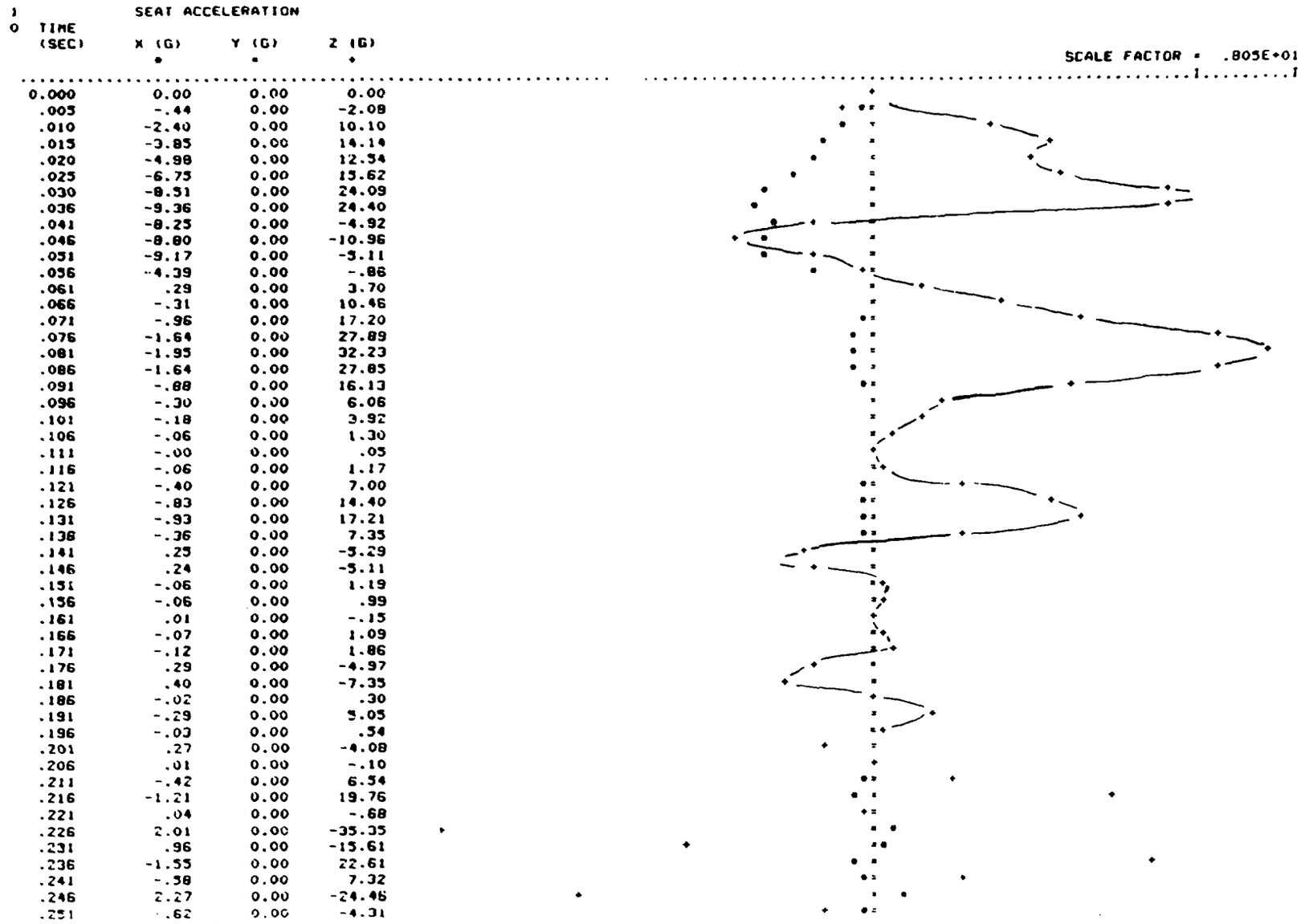

SEAT ACCELERATION

TIME (SEC)	X (G)	Y (G)	Z (G)
0.000	0.00	0.00	0.00
.005	-.44	0.00	-2.08
.010	-2.40	0.00	10.10
.015	-3.85	0.00	14.14
.020	-4.98	0.00	12.54
.025	-6.75	0.00	15.62
.030	-8.51	0.00	24.09
.036	-9.36	0.00	24.40
.041	-8.25	0.00	-4.92
.046	-8.80	0.00	-10.96
.051	-9.17	0.00	-5.11
.056	-4.39	0.00	-.86
.061	.29	0.00	3.70
.066	-.31	0.00	10.46
.071	-.96	0.00	17.20
.076	-1.64	0.00	27.89
.081	-1.95	0.00	32.23
.086	-1.64	0.00	27.85
.091	-.88	0.00	16.13
.096	-.30	0.00	6.06
.101	-.18	0.00	3.92
.106	-.06	0.00	1.30
.111	-.00	0.00	.05
.116	-.06	0.00	1.17
.121	-.40	0.00	7.00
.126	-.83	0.00	14.40
.131	-.93	0.00	17.21
.136	-.36	0.00	7.35
.141	.25	0.00	-5.29
.146	.24	0.00	-5.11
.151	-.06	0.00	1.19
.156	-.06	0.00	.99
.161	.01	0.00	-.15
.166	-.07	0.00	1.09
.171	-.12	0.00	1.86
.176	.29	0.00	-4.97
.181	.40	0.00	-7.35
.186	-.02	0.00	.30
.191	-.29	0.00	5.05
.196	-.03	0.00	.54
.201	.27	0.00	-4.08
.206	.01	0.00	-.10
.211	-.42	0.00	6.54
.216	-1.21	0.00	19.76
.221	.04	0.00	-.68
.226	2.01	0.00	-35.35
.231	.96	0.00	-15.61
.236	-1.55	0.00	22.61
.241	-.58	0.00	7.32
.246	2.27	0.00	-24.46
.251	.62	0.00	-4.31

Figure 20. Case S3F simulation of seat bucket acceleration.

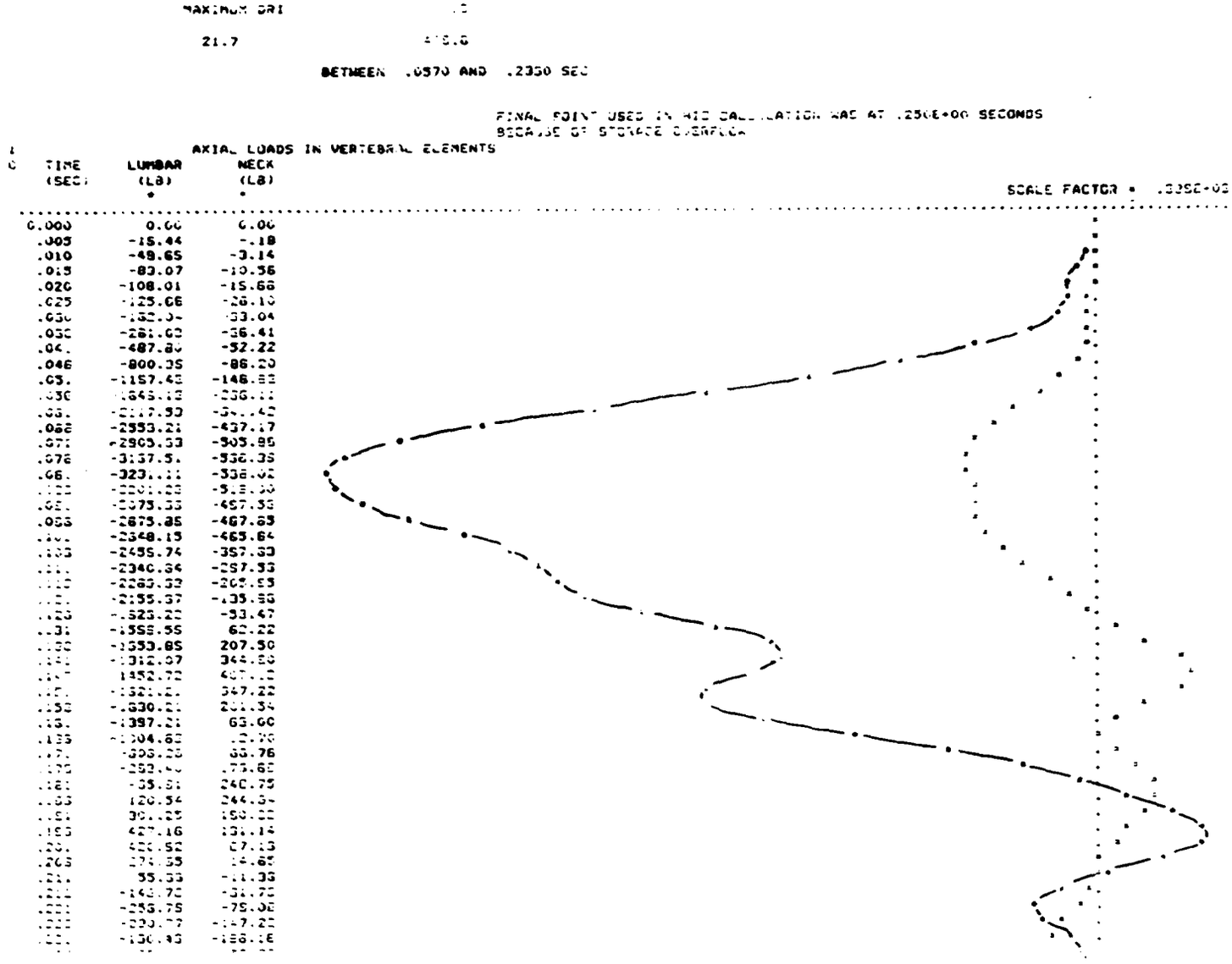

Figure 21. Case S3F simulation of *lumbar loads*. Conditions: constant acceleration of SH-60B Seahawk seat bucket with heavy occupant.

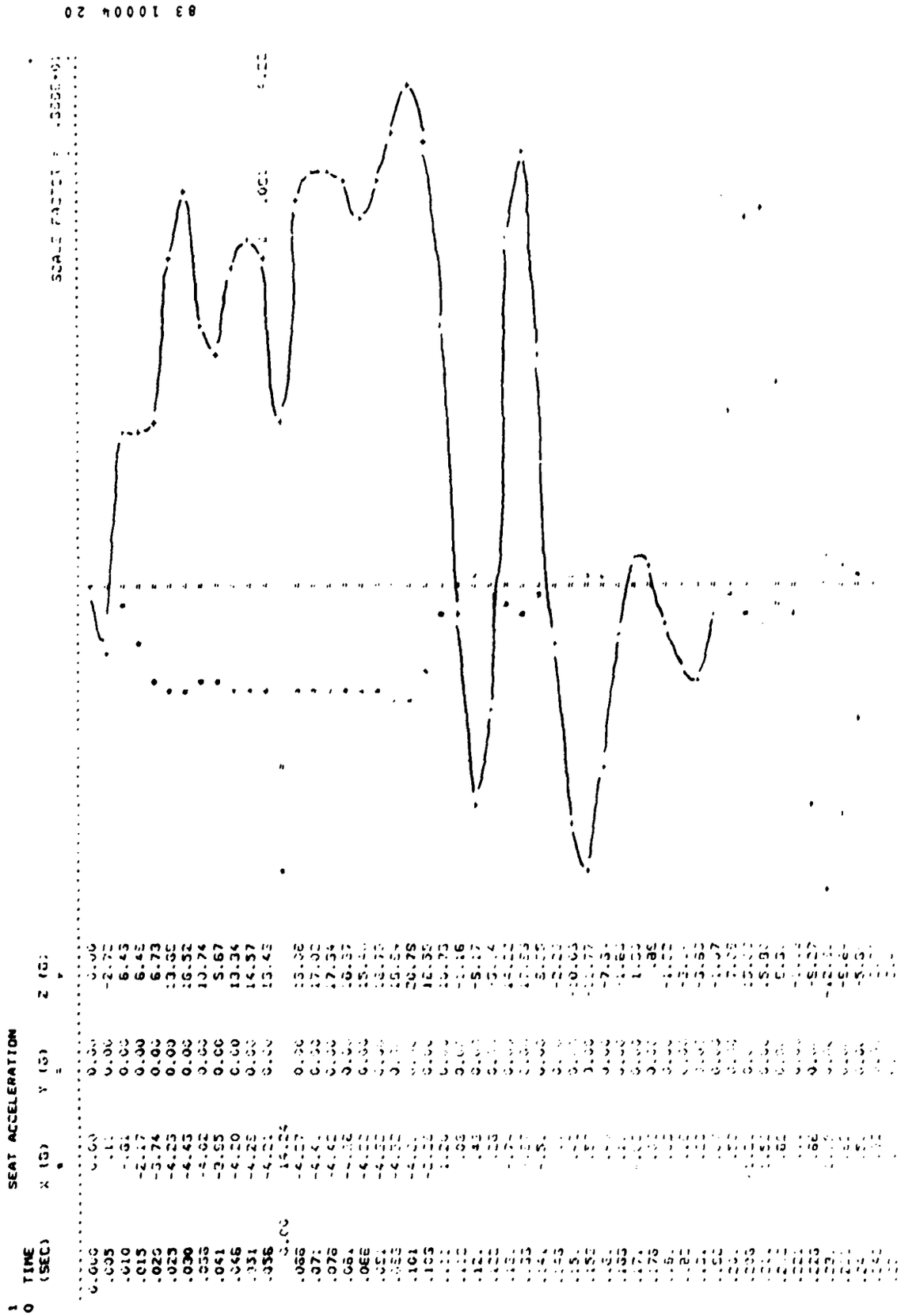

Figure 22. Case S3A simulation of seat bucket acceleration.

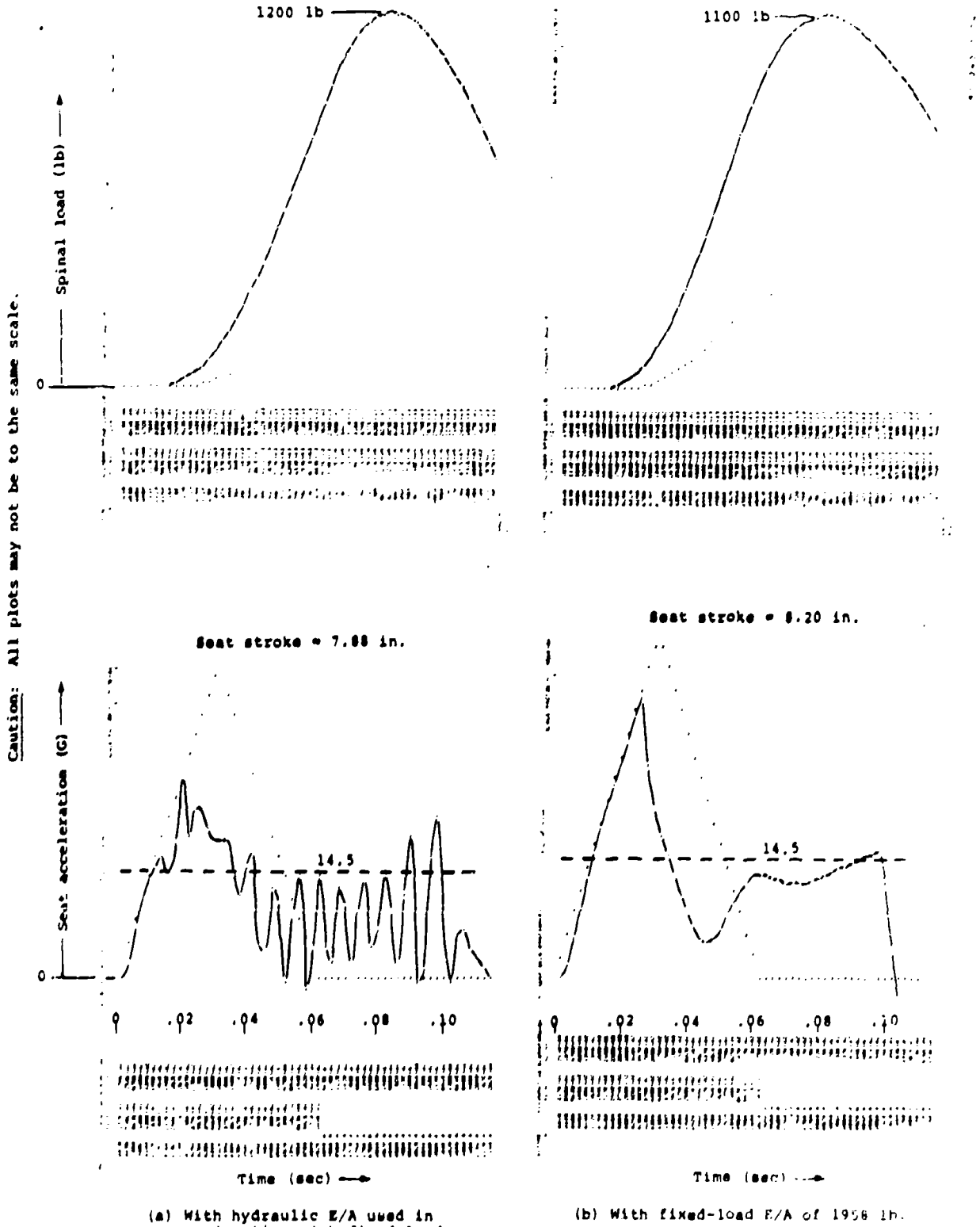

(a) With hydraulic E/A used in conjunction with fixed-load E/A of 1350 lb.

(b) With fixed-load E/A of 1950 lb.

Figure 23. Computer simulation of distributed mass system composed of 5th-percentile occupant in a 23-lb bucket.

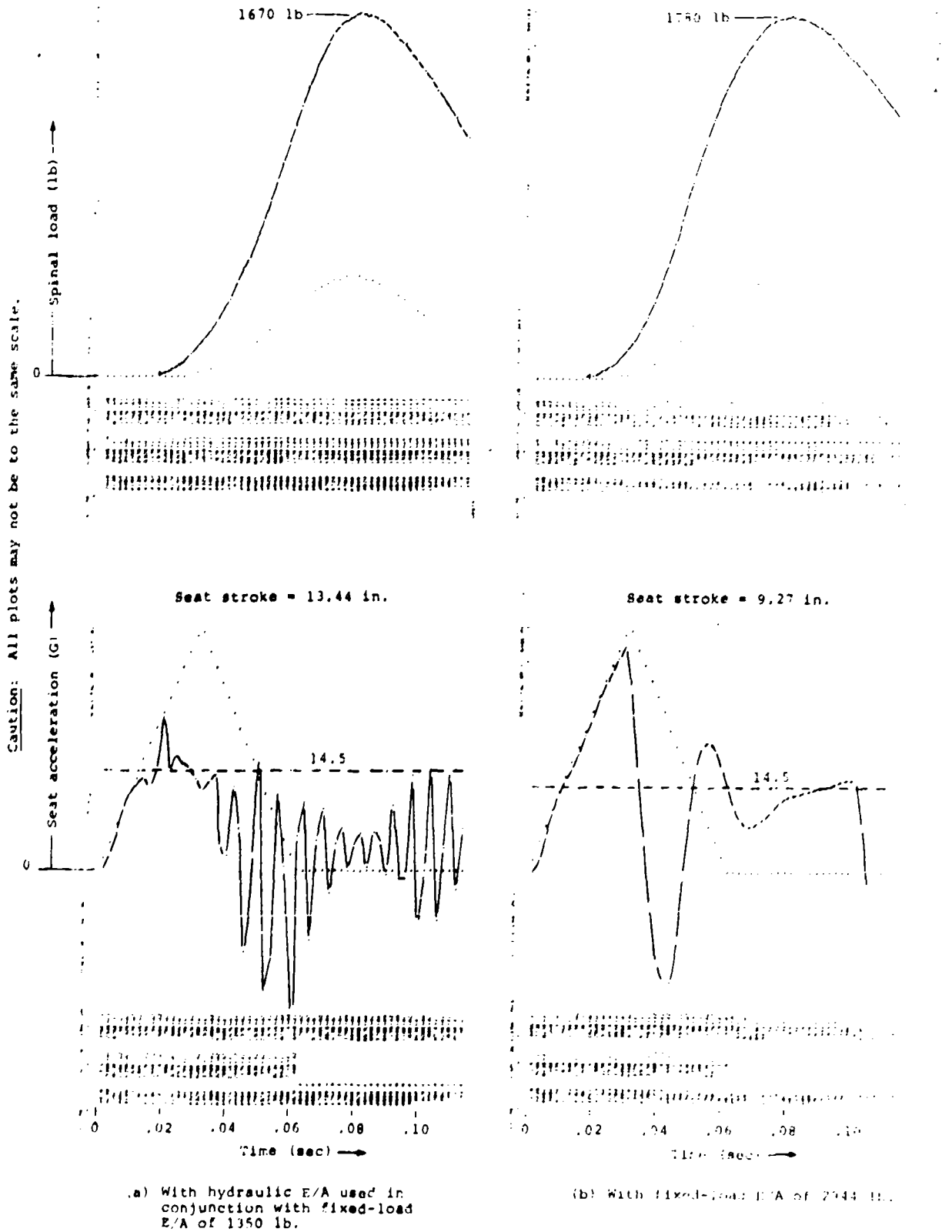

(a) With hydraulic E/A used in conjunction with fixed-load E/A of 1350 lb.

(b) With fixed-load E/A of 2044 lb.

Figure 24. Computer simulation of distributed mass system composed of 95th-percentile occupant in a 23-lb bucket.

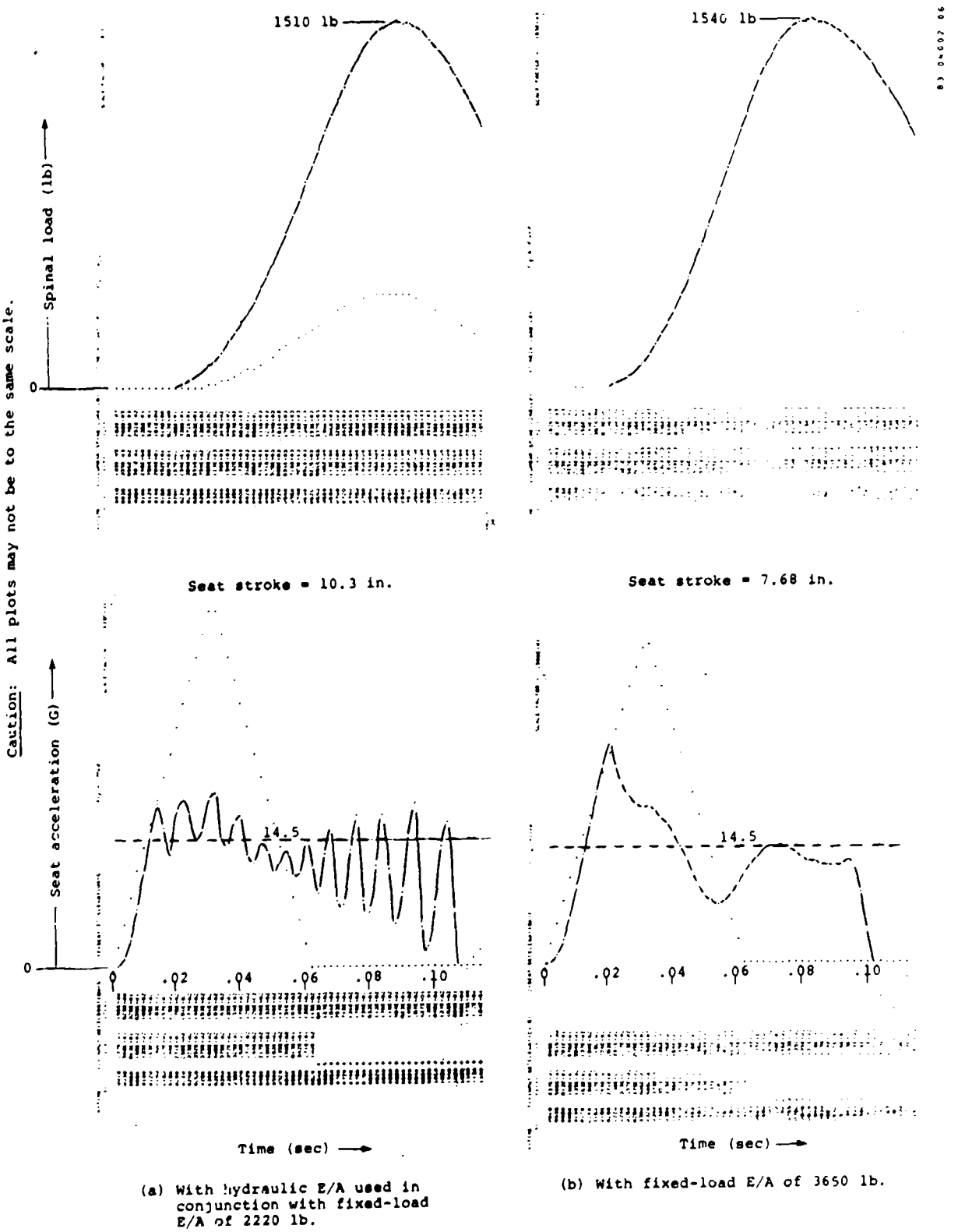

(a) With hydraulic E/A used in conjunction with fixed-load E/A of 2220 lb.

(b) With fixed-load E/A of 3650 lb.

Figure 25. Computer simulation of distributed mass system composed of 50th-percentile occupant in a 110-lb bucket.

TABLE 6. SIZE AND WEIGHT COMPARISON

Factor	System Type ASAVLEA	MAVLEA
Size (in.)		
• Overall length for 16-in. stroke	25.0	11.0
• Maximum diameter	1.5*	1.86
• Typical diameter	1.35*	1.5
Weight (lb)		
• Hydraulic energy absorber	2.6	-
• Companion fixed-load energy absorber	0.8	-
• Variable-load energy absorber (two at 1.0 lb each)	-	2.0
• Remote control hardware	-	1.0
Total Weight	3.4	3.0

*Companion fixed-load energy absorber is 1.5-in. diameter.

In crash conditions, which would require the hydraulic energy absorber to contribute load, the reliability of the hydraulic energy absorber must be considered. Freedom from failure depends mostly upon the proper functioning of the automatic relief valve. The simplicity of the valve is one factor contributing to its reliability. Another factor is the filters which prevent contaminants from entering the tiny passages in the first stage. Filters on the outlet as well as the inlet to the first stage are necessary because during operational use or storage, temperature changes would cause fluid to enter the outlet.

Gas within the hydraulic energy absorber can temporarily delay application of the required load unless that gas is confined to the low pressure side of the piston. The gas which is required to accommodate the thermal expansion of the hydraulic fluid must therefore be enclosed in a bladder. For high system reliability, the integrity of the bladder and other seals between the fluid and the atmosphere must also be high.

If, during crash conditions, a failure of the hydraulic energy absorber were to occur, the degree of failure is limited by the low and high limits on the load. The low limit of the combined hydraulic energy absorber and companion fixed-load energy absorber would be the load of the total fixed-load energy absorber, and that which is approximately correct for the 5th-percentile occupant. At the other extreme, failure of the hydraulic energy absorber toward

an abnormally high load would be limited by the redundant safety relief valve, set for the load required for the 95th-percentile occupant. The potential limits of a failure of the ASAVLEA system are therefore approximately equivalent to those of a MAVLEA system.

Accuracy Comparison

Compared to the MAVLEA system, the ASAVLEA system offers the potential for greater accuracy by avoiding adjustment errors and by automatically compensating for unusual factors affecting seat bucket acceleration. One such factor might be the impact of a stroking seat bucket with a console or other obstruction. Another factor might be friction in the seat bucket guidance mechanisms. The ASAVLEA would automatically compensate for variations in friction as well as variations in occupant weight. Test results with lumped masses presented in "Test Conditions and Results" demonstrate the hydraulic energy absorber to be sufficiently accurate. When distributed mass systems are considered, the hydraulic energy absorber's performance is predicted by the computer simulations to be less accurate, but final conclusions must await the results of further testing.

Regardless of how accurately an energy-absorbing system controls the acceleration of a portion of a distributed mass system, the ultimate measure of performance is prevention of spinal injury. The positive correlation of seat bucket acceleration and spinal injury is unquestioned, but many other recognized factors also affect injury. Among these factors are: occupant age, bone structure and health, seated posture, weight ratio of occupant to seat bucket, seat elasticity, cushion rigidity, restraint system effectiveness, and the acceleration-time history of the crash input. All these factors interact with the energy absorber load to determine whether compressive and bending loads in the spine reach the fracture limit. Ideal energy absorber accuracy is an elusive goal, requiring consideration of the overall system as well as the accuracy of seat bucket acceleration.

Cost Effectiveness

For purpose of comparison, the total price per seat of the ASAVLEA is estimated to be 40 percent greater than the MAVLEA. Estimates are based upon a 200-seat production lot, and tooling is not included in the piece price. The ASAVLEA system includes a fixed-load inversion tube energy absorber as well as the hydraulic energy absorber. The MAVLEA includes two variable-load energy absorbers with associated control dial and control cables.

Maintenance

With the automatic relief valve built into the piston, the hydraulic energy absorber would require no maintenance. Furthermore, there would be no opportunity for tampering or readjustment without disassembly. Shelf and operational life would be limited only by the life of seals retaining fluid, and visual inspection for external leakage would be the only required periodic inspection.

The MAVLEA of Reference 4 would require the same amount of maintenance (none) but would require periodic inspection of the control dial and cables.

CONCLUSIONS AND RECOMMENDATIONS

The acceleration-sensing automatic variable-load energy absorber (ASAVLEA) demonstrated its ability to provide a predetermined constant deceleration to any lumped mass ranging from 135 to 223 lb and to account for other variables such as seat interference with consoles during stroking, a feature not possible with fixed load or manually adjustable variable-load energy absorber (MAVLEA) systems. Other analyses of the ASAVLEA suggest that its reliability, maintainability, size, weight, and cost effectiveness are competitive with MAVLEA systems.

A question remains as to whether the ASAVLEA will be effective in preventing injurious spinal loads in a distributed mass system such as that represented by an anthropomorphic dummy. Testing of the response of such a distributed mass system must be performed before final conclusions can be made concerning feasibility of the ASAVLEA.

REFERENCES

1. MIL-S-81771A(AS) - MILITARY SPECIFICATION, SEATS, AIRCREW, ADJUSTABLE; AIRCRAFT, GENERAL SPECIFICATION FOR, Washington, D.C., 30 April 1975.

2. Desjardins, S. P., and Laananen, D. H., AIRCRAFT CRASH SURVIVAL DESIGN GUIDE, Volume IV, AIRCRAFT SEATS, RESTRAINTS, LITTERS, AND PADDING, Simula Inc.; USARTL-Technical Report 79-22D, Applied Technology Laboratory, U.S. Army Research and Technology Laboratories (AVRADCOM), Fort Eustis, Virginia, June 1980.

3. CRASH SURVIVAL DESIGN GUIDE, Dynamic Science, Division of Marshall Industries; USAAMRDL Technical Report 71-22, Fort Eustis Directorate, U.S. Army Air Mobility Research and Development Laboratory, Fort Eustis, Virginia, October 1971.

4. Svoboda, C. M., and Warrick, J. C., DESIGN AND DEVELOPMENT OF VARIABLE-LOAD ENERGY ABSORBERS, NAVAIRDEVCEN Technical Report No. NADC-81302-60, Naval Air Development Center, Warminster, Pennsylvania, February 1981.

APPENDIX A

SAMPLE COMPUTER OUTPUT

***** PROGRAM VHEAD INPUT DATA *****

5TH PERCENTILE LUMPED MASS.23LB BUCKET 4/4/83.RUN NO.2

FLOW AREAS= .98175 .39270 .32398 .30680 0.00000 .22936 .43982 .00785 .00082 .69398
.00283 0.00000 .00312 .01767 .17349 0.00000 .00750

MAIN VALVE SPRING RATE=		72.000							
AMPLIFIER VALVE SPRING RATE=		240.000							
MASSES=		.349375	.000518	.000128					
FLUID IMPULSE FORCE ANGLE=		45.00							
PRESSURE-COMPENSATED FLOW RATE=		2.00							
ATMOSPHERIC PRESSURE=		14.700							
ORIFICE COEFFICIENTS=	0.000	.670	-0.000	-0.000	.660	-0.000	-0.000	.610	.620
	-0.000	.800	.690	.800	.600	-0.000	-0.000	.680	
NUMBER OF EA SETS=		1							
INVERTED TUBE EA LIMIT LOAD=		1350.000							
PRELOAD DISTANCE FOR MAIN VALVE=		.10000							
WIDTH OF MAIN VALVE OPENING= PI *		.625							
PRELOAD DISTANCE FOR INERTIAL VALVE=		.00900							
WIDTH OF INERTIAL VALVE OPENING= 2 *		.250							
FLUID MASS DENSITY=		.0000825							
GRAVITATIONAL CONSTANT=		386.40							
FLUID COMPRESSIBILITY FACTOR=		.175E+06							
MAX INTEGRATION TIME STEP=		.000250							
MIN INTEGRATION TIME STEP=		.000250							
UPPER REL ERROR BOUND=		.05000							
LOWER REL ERROR BOUND=		.00100							
FINAL INTEGRATION TIME=		.120							
INITIAL AIRCRAFT VELOCITY=		0.000							

TIME	P(1)	P(3)	P(5)	P(7)	P(8)	P(9)	P(10)	Q(1)	Q(3)	Q(4)	Q(5)	Q(7)	Q(8)	Q(9)	A(5)	A(12)
.00175	18.68	18.68	14.70	17.78	17.78	17.78	14.70	.02	.00	.02	.02	0.00	0.00	.00	.000000	.000100
.00375	52.55	52.55	14.70	49.54	49.54	48.54	14.70	.06	.00	.06	.06	0.00	0.00	.00	.000000	.000100
.00600	159.65	158.65	14.70	153.66	153.65	153.65	14.70	.12	.00	.12	.12	0.00	0.00	.00	.000001	.000100
.00800	329.67	328.67	14.70	320.78	320.77	320.77	14.70	.18	.00	.18	.18	0.00	0.00	.00	.000002	.000100
.01000	564.18	564.18	14.70	552.41	552.40	552.40	14.70	.24	.01	.24	.24	0.00	0.00	.01	.000002	.000100
.01200	838.88	838.86	14.70	785.18	784.97	785.58	14.70	1.08	.01	1.07	1.07	.20	0.00	.01	.000003	.000381
.01400	1055.04	1055.00	14.70	454.88	451.48	452.56	-1.55	14.30	11.38	2.00	4.09	.26	1.17	10.21	.003655	.001980
.01600	751.92	751.31	14.93	319.98	316.14	315.82	-1.51	50.07	47.14	2.00	4.11	-.13	1.18	45.96	.018310	.002462
.01800	331.51	331.15	14.86	145.32	145.09	143.34	18.64	36.40	34.86	2.00	.95	-.33	-.59	35.45	.020954	.000853
.02000	392.56	392.51	14.72	178.79	178.79	178.88	29.11	21.79	20.62	2.00	.13	.08	-1.05	21.67	.011250	.000100
.02200	84[illegible]4	46.10	14.71	371.60	370.70	371.68	14.66	15.43	13.39	2.00	2.09	.25	.05	13.34	.004825	.001106
.02400	1259.30	1259.02	14.73	539.41	533.28	533.68	-10.78	54.43	50.98	2.00	5.28	.15	1.83	49.15	.015221	.002407
.02600	930.01	928.28	15.40	396.27	391.68	391.24	-3.51	97.64	94.58	2.00	4.41	-.17	1.35	93.23	.033670	.002412
.02800	609.63	607.91	15.30	265.25	264.68	263.73	15.97	87.95	86.18	2.00	1.50	-.24	-.28	86.46	.038513	.000994
.03000	793.01	792.54	14.90	348.82	348.68	349.80	20.66	83.75	82.29	2.00	.78	.10	-.68	82.97	.032131	.000446
.03200	1189.41	1188.73	14.75	512.95	509.31	510.76	-.82	108.15	105.26	2.00	4.00	.30	1.12	104.14	.033211	.001900
.03400	1084.45	1089.54	16.78	462.67	455.56	455.55	-10.63	157.50	153.98	2.00	5.43	-.03	1.92	152.06	.051272	.002820
.03600	768.22	761.36	17.83	330.90	329.03	327.71	14.40	159.72	157.42	2.00	2.70	-.29	.39	157.03	.063502	.001635
.03800	808.09	802.98	17.58	352.88	352.61	352.61	20.62	157.05	155.48	2.00	1.03	-.01	-.34	156.02	.061290	.000599
.04000	998.59	993.00	17.28	432.44	430.37	431.47	12.52	171.48	169.06	2.00	2.93	.26	.52	168.54	.059944	.001556
.04200	930.49	921.58	18.77	392.86	388.07	388.07	-.79	195.05	192.00	2.00	4.37	0.00	1.32	190.68	.071115	.002498
.04400	761.85	751.29	18.64	326.86	325.07	324.15	16.71	195.91	193.85	2.00	2.59	-.24	.33	193.32	.080209	.001614
.04600	786.88	777.43	18.21	340.80	340.42	340.41	20.82	193.21	191.57	2.00	1.19	-.01	-.45	192.02	.078412	.000722
.04800	875.17	866.78	18.65	378.01	376.35	377.06	18.54	198.59	197.35	2.00	2.54	.21	.30	197.05	.076847	.001486
.05000	803.88	794.03	19.27	340.04	336.75	336.75	6.81	207.36	204.69	2.00	3.50	0.00	.84	203.86	.084010	.002210
.05200	701.86	691.79	18.52	301.42	300.13	299.50	19.11	202.69	200.63	2.00	2.13	-.20	.07	200.56	.089143	.001427
.05400	717.52	709.35	18.67	310.00	309.65	309.65	20.29	196.07	194.46	2.00	1.12	0.00	-.49	194.96	.086039	.000738
.05600	752.44	746.18	17.61	324.73	323.43	323.90	17.25	194.12	192.05	2.00	2.16	.17	.09	191.97	.083594	.001417
.05800	682.77	676.65	17.47	291.20	289.02	289.01	12.57	190.61	188.29	2.00	2.72	-.03	.40	187.88	.087198	.001937
.06000	610.29	605.13	17.11	262.48	261.66	261.20	17.86	179.58	177.76	2.00	1.59	-.17	-.23	177.99	.088367	.001203
.06200	611.86	609.84	15.59	265.04	264.79	264.80	18.29	167.34	165.84	2.00	.89	.02	-.62	166.48	.083286	.000673
.06400	604.81	603.82	14.88	261.19	260.35	260.64	15.73	158.18	156.33	2.00	1.65	.14	-.19	156.53	.079041	.001272
.06600	544.00	543.05	14.81	233.91	232.70	232.67	14.95	147.94	145.87	2.00	1.93	-.04	-.04	146.01	.078711	.001610
.06800	498.37	497.63	14.88	214.29	213.90	213.58	15.53	135.52	133.93	2.00	1.08	-.14	-.52	134.44	.075955	.000934
.07000	497.88	497.28	14.91	217.29	217.16	217.16	20.53	123.85	122.45	2.00	.64	.02	-.76	123.21	.068869	.000539
.07200	497.25	496.66	14.84	214.71	214.24	214.44	15.82	114.26	112.39	2.00	1.25	.11	-.42	113.01	.062824	.001060
.07400	458.40	457.86	14.80	197.71	196.98	196.97	15.81	104.61	102.82	2.00	1.52	-.03	-.27	103.09	.059962	.001355
.07600	425.64	425.22	14.82	184.52	184.27	184.04	17.62	93.24	91.74	2.00	.87	.12	-.63	92.37	.055479	.000801
.07800	433.17	432.84	14.82	191.28	191.21	191.21	22.98	82.01	80.88	2.00	.48	.01	-.85	81.53	.047524	.000424
.08000	449.37	449.08	14.79	195.65	195.37	195.55	17.23	72.56	71.00	2.00	1.01	.11	-.55	71.55	.040260	.000864
.08200	420.65	420.39	14.76	182.09	181.54	181.54	15.26	63.85	62.12	2.00	1.38	0.00	-.34	62.46	.036228	.001225
.08400	380.62	380.44	14.76	166.60	166.40	166.18	18.72	53.03	51.54	2.00	.85	-.12	-.64	52.19	.031416	.000776
.08600	396.66	396.54	14.75	177.82	177.78	177.78	25.28	41.13	39.86	2.00	.35	-.02	-.92	40.77	.023115	.000302
.08800	471.19	471.11	14.73	207.97	207.79	208.03	19.46	30.40	28.90	2.00	.88	.12	-.62	29.52	.014797	.000689
.09000	485.12	485.05	14.71	211.76	211.06	211.11	14.86	24.57	22.69	2.00	1.73	.05	-.15	22.84	.011287	.001290
.09200	352.96	352.92	14.71	154.65	154.32	154.03	16.97	16.77	15.13	2.00	1.18	-.14	-.46	15.59	.008847	.001035
.09400	274.77	274.76	14.70	127.05	127.05	126.76	28.71	2.79	1.62	2.00	.14	-.13	-1.04	2.66	.001037	.000127
.09600	213.52	213.52	14.70	200.40	200.39	200.45	14.70	.80	.54	.26	.26	.06	0.00	.54	.000393	.000190
.09800	-110.07	-109.72	14.70	-52.82	-52.82	-52.82	10.93	-1.54	-.87	-1.14	-.08	0.00	.59	-1.46	.000808	.000100
.10000	-246.01	-238.72	14.68	-118.36	-118.36	-118.36	-3.19	-18.86	-18.47	-2.41	-.11	0.00	1.28	-19.75	.012931	.000100
.10200	-104.52	-99.37	14.88	-49.79	-49.79	-49.79	10.13	-19.70	-19.11	-.99	-.07	0.00	.51	-19.63	.021623	.000100
.10400	-60.33	-56.68	14.69	-29.36	-29.36	-29.36	13.28	-17.21	-16.88	-.55	-.06	0.00	.27	-17.15	.025352	.000100
.10600	-32.64	-30.28	14.68	-17.18	-17.18	-17.18	14.36	-13.98	-13.81	-.26	-.05	0.00	.12	-13.93	.027294	.000100
.10800	-6.55	-5.61	14.70	-6.10	-6.10	-6.10	14.71	-8.81	-8.80	.01	-.04	0.00	-.03	-8.77	.027689	.000100
.11000	12.27	12.27	14.70	1.95	1.95	1.95	14.90	-2.29	-2.39	.21	-.03	0.00	-.13	-2.26	.026762	.000100
.11200	20.34	20.34	14.70	5.76	5.76	5.76	15.18	3.87	3.82	.29	-.04	0.00	-.18	4.01	.025148	.000100
.11400	41.35	41.35	14.70	15.51	15.51	15.51	15.78	9.18	8.89	.52	.00	0.00	-.29	9.18	.022783	.000100
.11600	75.33	75.32	14.71	31.93	31.92	31.92	17.94	12.64	12.14	.87	.03	0.00	-.47	12.60	.018973	.000100
.11800	130.81	130.79	14.71	59.56	59.56	59.56	22.95	13.11	12.29	1.42	.06	0.00	-.76	13.05	.012915	.000100
.12000	280.11	280.10	14.70	129.70	129.70	129.70	29.42	6.03	4.86	2.00	.11	0.00	-1.06	5.92	.003126	.000100

TIME	X1	X1DOT	X1DDOT	X2	X2DOT	X2DDOT	X3	X3DOT	X3DDOT	X4	X4DOT	X4DDOT
.00175	.0005	.802	918.51	.0000	.013	29.32	.0000	.013	29.32	.0000	.013	29.05
.00375	.0046	3.682	1863.50	.0002	.263	276.93	.0002	.263	276.93	.0002	.263	276.14
.00600	.0189	8.425	3141.37	.0020	1.648	1058.32	.0020	1.648	1058.32	.0020	1.648	1056.80
.00800	.0447	16.755	4188.38	.0082	4.915	2296.74	.0082	4.815	2296.74	.0082	4.915	2294.51
.01000	.0873	26.179	5235.38	.0237	11.145	4002.85	.0237	11.145	4002.85	.0237	11.145	3999.92
.01200	.1508	37.696	6282.35	.0553	21.125	6008.55	.0545	19.953	5115.34	.0553	21.125	6004.98
.01400	.2395	51.309	7329.35	.1103	34.160	6787.32	.1063	32.675	7446.67	.1122	37.172	6819.33
.01600	.3575	67.014	8376.34	.1920	47.236	5935.58	.1871	47.992	7245.77	.2013	50.272	6835.38
.01800	.5090	84.813	9423.34	.2974	57.788	4754.22	.2957	59.885	4508.48	.3081	56.271	6835.36
.02000	.6981	104.707	10470.33	.4224	67.304	4925.77	.4223	66.950	4298.40	.4282	64.604	6835.36
.02200	.9292	126.685	11517.33	.5676	78.304	6200.34	.5654	76.875	6022.72	.5701	78.428	6835.36
.02400	1.2083	150.776	12564.32	.7377	92.174	7361.30	.7329	91.290	8002.99	.7454	96.900	7520.86
.02600	1.5337	176.952	13611.31	.9366	106.408	6436.02	.9317	107.383	7288.79	.9536	109.883	7544.74
.02800	1.9155	205.222	14658.31	1.1616	118.281	5535.74	1.1596	119.661	9061.58	1.1811	117.555	7544.74
.03000	2.3560	235.585	15705.30	1.4095	129.814	6051.04	1.4086	129.238	4799.11	1.4258	128.055	7544.74
.03200	2.8591	267.519	15705.30	1.6821	143.272	7164.91	1.6783	141.552	7486.06	1.6989	148.157	7544.74
.03400	3.4248	297.883	14658.31	1.9834	157.919	6898.07	1.9778	158.105	8108.79	2.0083	162.868	7680.33
.03600	4.0482	326.153	13611.31	2.3125	170.898	5981.38	2.3093	172.549	5807.64	2.3448	171.903	7680.33
.03800	4.7280	352.328	12564.32	2.6664	183.039	6095.63	2.6652	183.110	4951.42	2.6976	181.645	7680.33
.04000	5.4571	376.410	11517.33	3.0453	196.066	6628.72	3.0422	194.556	6682.85	3.0757	197.412	7680.33
.04200	6.2323	398.398	10470.33	3.4510	209.601	6437.35	3.4480	209.564	7453.89	3.4870	213.011	7680.33
.04400	7.0493	418.291	9423.34	3.8839	222.225	5962.91	3.8798	223.606	5884.68	3.9237	223.071	7680.33
.04600	7.9040	436.091	8376.34	4.3396	234.427	6033.24	4.3382	234.506	5088.41	4.3795	233.280	7680.33
.04800	8.7923	451.797	7329.35	4.8210	247.117	6281.91	4.8180	245.904	6338.79	4.8600	247.901	7680.33
.05000	9.7098	465.408	6282.35	5.3281	259.931	6081.57	[illegible]	259.979	6922.42	5.3707	262.092	7680.33
.05200	10.6525	478.926	5235.36	5.8602	272.119	5794.92	5.8574	273.262	5684.38	5.9055	272.305	7680.33
.05400	11.6161	486.350	4188.36	6.4164	284.071	5838.91	6.4149	284.047	5071.21	6.4601	282.800	7680.33
.05600	12.5965	493.679	3141.37	6.9967	296.300	5937.05	6.9938	295.316	6058.18	7.0390	296.524	7680.33
.05800	13.5894	498.915	2094.38	7.6015	308.466	5741.26	7.5976	308.628	6449.79	7.6456	308.505	7680.33
.06000	14.5907	502.057	1047.38	8.2301	320.148	5537.60	8.2277	321.111	5402.15	8.2750	319.563	7680.33
.06200	15.5962	503.105	.39	8.8819	331.659	5542.02	8.8806	331.556	4946.84	8.9242	330.058	7680.33
.06400	16.6023	503.105	0.00	9.5568	343.243	5522.20	9.5542	342.463	5722.14	9.5968	342.741	7680.33
.06600	17.6087	503.105	0.00	10.2547	354.601	5351.33	10.2514	354.858	5951.77	10.2945	354.507	7680.33
.06800	18.6149	503.105	0.00	10.9749	365.599	5223.11	10.9730	366.389	5091.54	11.0134	364.288	7680.33
.07000	19.6211	503.105	0.00	11.7169	376.446	5221.72	11.7158	376.305	4770.54	11.7519	374.483	7680.33
.07200	20.6273	503.105	0.00	12.4806	387.293	5219.94	12.4785	386.639	5411.22	12.5125	386.212	7680.33
.07400	21.6335	503.105	0.00	13.2659	398.002	5110.79	13.2632	398.188	5640.97	13.2963	397.309	7680.33
.07600	22.6397	503.105	0.00	14.0724	408.449	5018.73	14.0708	409.133	4958.58	14.1005	406.826	7680.33
.07800	23.6459	503.105	0.00	14.8996	418.792	5039.88	14.8988	418.724	4636.54	14.9238	416.608	7690.33
.08000	24.6521	503.105	0.00	15.7476	429.198	5085.42	15.7459	428.572	5187.52	15.7680	427.777	7680.33
.08200	25.6583	503.105	0.00	16.6164	439.550	5004.72	16.6138	439.595	5506.76	16.6347	438.662	7680.33
.08400	26.6646	503.105	0.00	17.5056	449.639	4892.23	17.5040	450.315	4934.81	17.5215	447.979	7880.33
.08600	27.6708	503.105	0.00	18.4148	459.602	4937.29	18.4142	459.699	4503.21	18.4265	457.230	7680.33
.08800	28.6770	503.105	0.00	19.3441	469.797	5146.74	19.3428	469.079	5021.81	19.3516	468.189	7680.33
.09000	29.6832	503.105	0.00	20.2942	480.295	5185.86	20.2916	479.987	5680.58	20.2999	479.909	7680.33
.09200	30.6894	503.105	0.00	21.2650	490.401	4814.51	21.2630	491.188	5206.31	21.2695	489.218	7680.33
.09400	31.6956	503.105	0.00	22.2553	499.763	4594.78	22.2550	500.527	4211.44	22.2558	497.077	7680.33
.09600	32.7018	503.105	0.00	23.2640	508.858	4278.53	23.2636	508.493	4416.98	23.2640	508.858	7680.33
.09800	33.7080	503.105	0.00	24.2893	515.935	2629.68	24.2883	515.935	2629.68	24.2887	517.455	7680.33
.10000	34.7142	503.105	0.00	25.3252	519.415	1101.27	25.3252	519.415	1101.27	25.3317	522.727	7680.33
.10200	35.7204	503.105	0.00	26.3656	520.672	178.01	26.3656	520.672	178.01	26.3765	521.998	7680.33
.10400	36.7266	503.105	0.00	27.4064	519.760	-1036.06	27.4064	519.760	-1036.06	27.4193	520.465	7680.33
.10600	37.7329	503.105	0.00	28.4431	516.493	-2133.41	28.4431	516.493	-2133.41	28.4569	516.801	7680.33
.10800	38.7391	503.105	0.00	29.4712	511.349	-2905.91	29.4712	511.349	-2905.91	29.4852	511.278	7680.33
.11000	39.7453	503.105	0.00	30.4877	505.095	-3252.88	30.4877	505.095	-3252.88	30.5013	504.750	7680.33
.11200	40.7515	503.105	0.00	31.4914	498.627	-3132.42	31.4914	498.627	-3132.42	31.5042	498.152	7680.33
.11400	41.7577	503.105	0.00	32.4828	492.939	-2499.16	32.4828	492.939	-2498.16	32.4944	492.198	7680.33
.11600	42.7639	503.105	0.00	33.4643	488.969	-1450.86	33.4643	488.969	-1450.96	33.4740	487.766	7680.33
.11800	43.7701	503.105	0.00	34.4402	487.402	-124.92	34.4402	487.402	-124.92	34.4469	485.437	7680.33
.12000	44.7763	503.105	0.00	35.4158	488.716	1477.75	35.4158	488.716	1477.75	35.4174	485.988	7680.33

X-TIME X(.)	Y1=MAIN PRESSURE(PSI) Y1(*)	Y2=AMPLIFIER PRESSURE(PSI) Y2(=)
.0018	.187E+02	.170E+02
.0038	.525E+02	.495E+02
.0060	.160E+03	.154E+03
.0080	.330E+03	.321E+03
.0100	.564E+03	.552E+03
.0120	.839E+03	.785E+03
.0140	.106E+04	.455E+03
.0160	.752E+03	.320E+03
.0180	.332E+03	.145E+03
.0200	.393E+03	.179E+03
.0220	.846E+03	.372E+03
.0240	.126E+04	.539E+03
.0260	.930E+03	.396E+03
.0280	.610E+03	.265E+03
.0300	.793E+03	.350E+03
.0320	.119E+04	.513E+03
.0340	.109E+04	.463E+03
.0360	.768E+03	.331E+03
.0380	.809E+03	.353E+03
.0400	.999E+03	.432E+03
.0420	.930E+03	.393E+03
.0440	.762E+03	.327E+03
.0460	.787E+03	.341E+03
.0480	.875E+03	.378E+03
.0500	.804E+03	.340E+03
.0520	.702E+03	.301E+03
.0540	.718E+03	.310E+03
.0560	.752E+03	.325E+03
.0580	.683E+03	.291E+03
.0600	.610E+03	.262E+03
.0620	.612E+03	.265E+03
.0640	.605E+03	.261E+03
.0660	.544E+03	.234E+03
.0680	.498E+03	.214E+03
.0700	.498E+03	.217E+03
.0720	.497E+03	.215E+03
.0740	.458E+03	.198E+03
.0760	.426E+03	.185E+03
.0780	.433E+03	.191E+03
.0800	.449E+03	.196E+03
.0820	.421E+03	.182E+03
.0840	.381E+03	.157E+03
.0860	.397E+03	.178E+03
.0880	.471E+03	.208E+03
.0900	.485E+03	.212E+03
.0920	.353E+03	.155E+03
.0940	.275E+03	.127E+03
.0960	.214E+03	.200E+03
.0980	-.110E+03	-.528E+02
.1000	-.246E+03	.118E+03
.1020	-.105E+03	-.498E+02
.1040	-.603E+02	-.294E+02
.1060	-.326E+02	-.172E+02
.1080	-.655E+01	-.610E+01
.1100	.1[illegible]3E+02	.195E+01
.1120	.203E+02	.576E+01
.1140	.414E+02	.155E+02
.1160	.753E+02	.319E+02
.1180	.131E+03	.596E+02
.1200	.[illegible]80E+03	.[illegible]30E+03

SCALE FACTOR = .160E+03

Fig 2

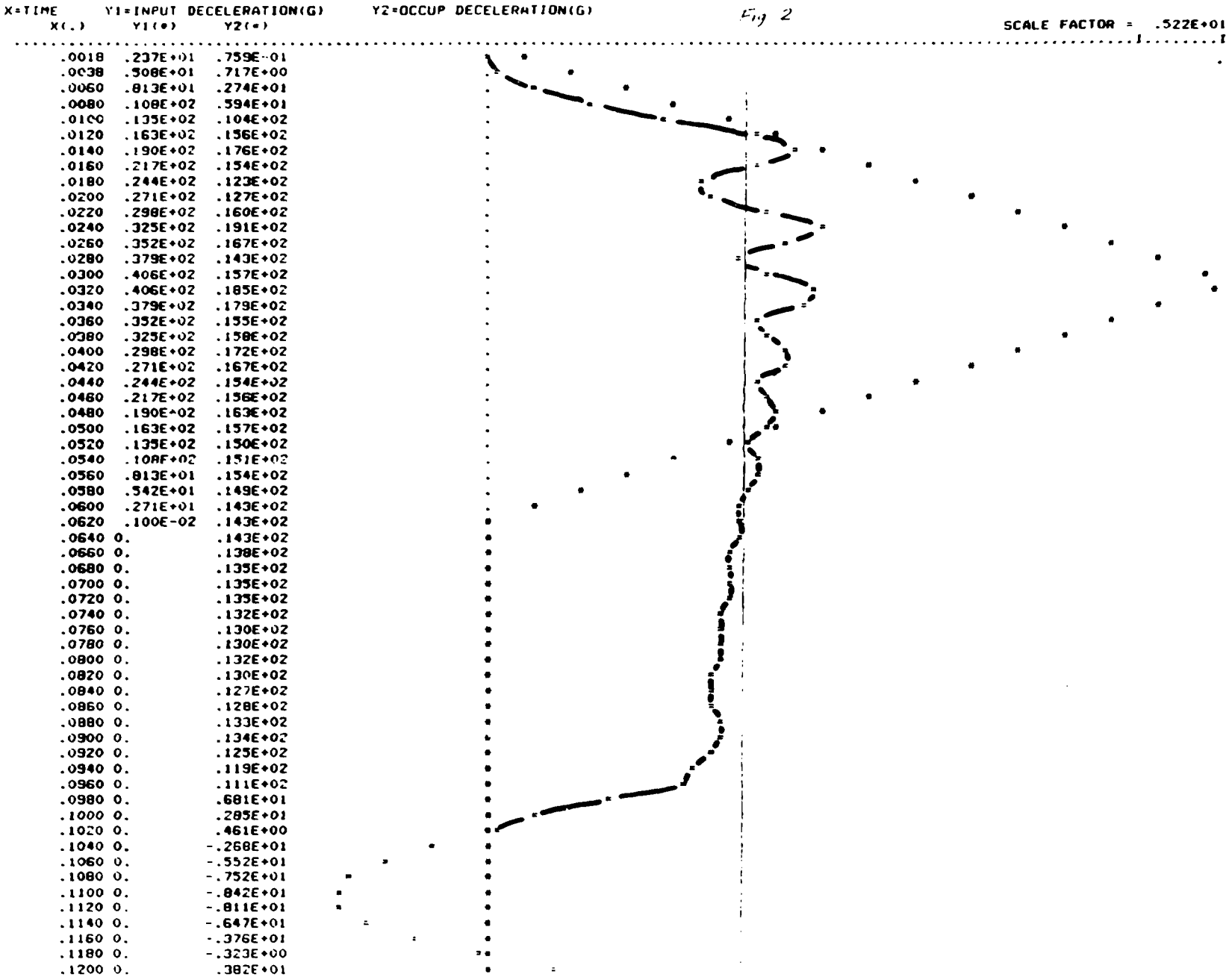
X=TIME
X(.)
Y1=INPUT DECELERATION(G)
Y1(*)
Y2=OCCUP DECELERATION(G)
Y2(*)
SCALE FACTOR = .522E+01
.0018 .237E+01 .759E-01
.0038 .508E+01 .717E+00
.0060 .813E+01 .274E+01
.0080 .108E+02 .594E+01
.0100 .135E+02 .104E+02
.0120 .163E+02 .156E+02
.0140 .190E+02 .176E+02
.0160 .217E+02 .154E+02
.0180 .244E+02 .123E+02
.0200 .271E+02 .127E+02
.0220 .298E+02 .160E+02
.0240 .325E+02 .191E+02
.0260 .352E+02 .167E+02
.0280 .379E+02 .140E+02
.0300 .406E+02 .157E+02
.0320 .406E+02 .185E+02
.0340 .379E+02 .179E+02
.0360 .352E+02 .155E+02
.0380 .325E+02 .158E+02
.0400 .298E+02 .172E+02
.0420 .271E+02 .167E+02
.0440 .244E+02 .154E+02
.0460 .217E+02 .156E+02
.0480 .190E+02 .163E+02
.0500 .163E+02 .157E+02
.0520 .135E+02 .150E+02
.0540 .108E+02 .151E+02
.0560 .813E+01 .154E+02
.0580 .542E+01 .149E+02
.0600 .271E+01 .143E+02
.0620 .100E-02 .143E+02
.0640 0. .143E+02
.0660 0. .138E+02
.0680 0. .135E+02
.0700 0. .135E+02
.0720 0. .135E+02
.0740 0. .132E+02
.0760 0. .130E+02
.0780 0. .130E+02
.0800 0. .132E+02
.0820 0. .130E+02
.0840 0. .127E+02
.0860 0. .128E+02
.0880 0. .133E+02
.0900 0. .134E+02
.0920 0. .125E+02
.0940 0. .119E+02
.0960 0. .111E+02
.0980 0. .681E+01
.1000 0. .285E+01
.1020 0. .461E+00
.1040 0. -.268E+01
.1060 0. -.552E+01
.1080 0. -.752E+01
.1100 0. -.842E+01
.1120 0. -.811E+01
.1140 0. -.647E+01
.1160 0. -.376E+01
.1180 0. -.323E+00
.1200 0. .382E+01

X=TIME Y1=REL DISP OF MAIN VALVE(IN) Y2=REL DISP OF INERTIAL VALVE(IN)

SCALE FACTOR = .481E-02

X(.)	Y1(*)	Y2(=)
.0018	0.	0.
.0038	0.	0.
.0060	0.	0.
.0080	0.	0.
.0100	0.	0.
.0120	0.	.762E-03
.0140	.185E-02	.396E-02
.0160	.929E-02	.492E-02
.0180	.107E-01	.171E-02
.0200	.573E-02	.165E-03
.0220	.244E-02	.221E-02
.0240	.769E-02	.481E-02
.0260	.171E-01	.482E-02
.0280	.196E-01	.199E-02
.0300	.163E-01	.891E-03
.0320	.168E-01	.380E-02
.0340	.259E-01	.564E-02
.0360	.322E-01	.327E-02
.0380	.312E-01	.120E-02
.0400	.304E-01	.311E-02
.0420	.360E-01	.500E-02
.0440	.407E-01	.323E-02
.0460	.389E-01	.144E-02
.0480	.380E-01	.297E-02
.0500	.425E-01	.442E-02
.0520	.452E-01	.285E-02
.0540	.437E-01	.148E-02
.0560	.424E-01	.283E-02
.0580	.441E-01	.387E-02
.0600	.448E-01	.241E-02
.0620	.423E-01	.135E-02
.0640	.400E-01	.254E-02
.0660	.398E-01	.322E-02
.0680	.385E-01	.187E-02
.0700	.350E-01	.108E-02
.0720	.318E-01	.212E-02
.0740	.303E-01	.271E-02
.0760	.281E-01	.160E-02
.0780	.242E-01	.848E-03
.0800	.204E-01	.173E-02
.0820	.183E-01	.245E-02
.0840	.159E-01	.155E-02
.0860	.118E-01	.603E-03
.0880	.750E-02	.134E-02
.0900	.570E-02	.258E-02
.0920	.448E-02	.207E-02
.0940	.528E-03	.255E-03
.0960	0.	.380E-03
.0980	.410E-03	0.
.1000	.651E-02	0.
.1020	.109E-01	0.
.1040	.128E-01	0.
.1060	.138E-01	0.
.1080	.141E-01	0.
.1100	.138E-01	0.
.1120	.128E-01	0.
.1140	.116E-01	0.
.1160	.970E-02	0.
.1180	.662E-02	0.
.1200	.159E-02	0.

RDY

APPENDIX B

REDUCED ENGINEERING DRAWINGS

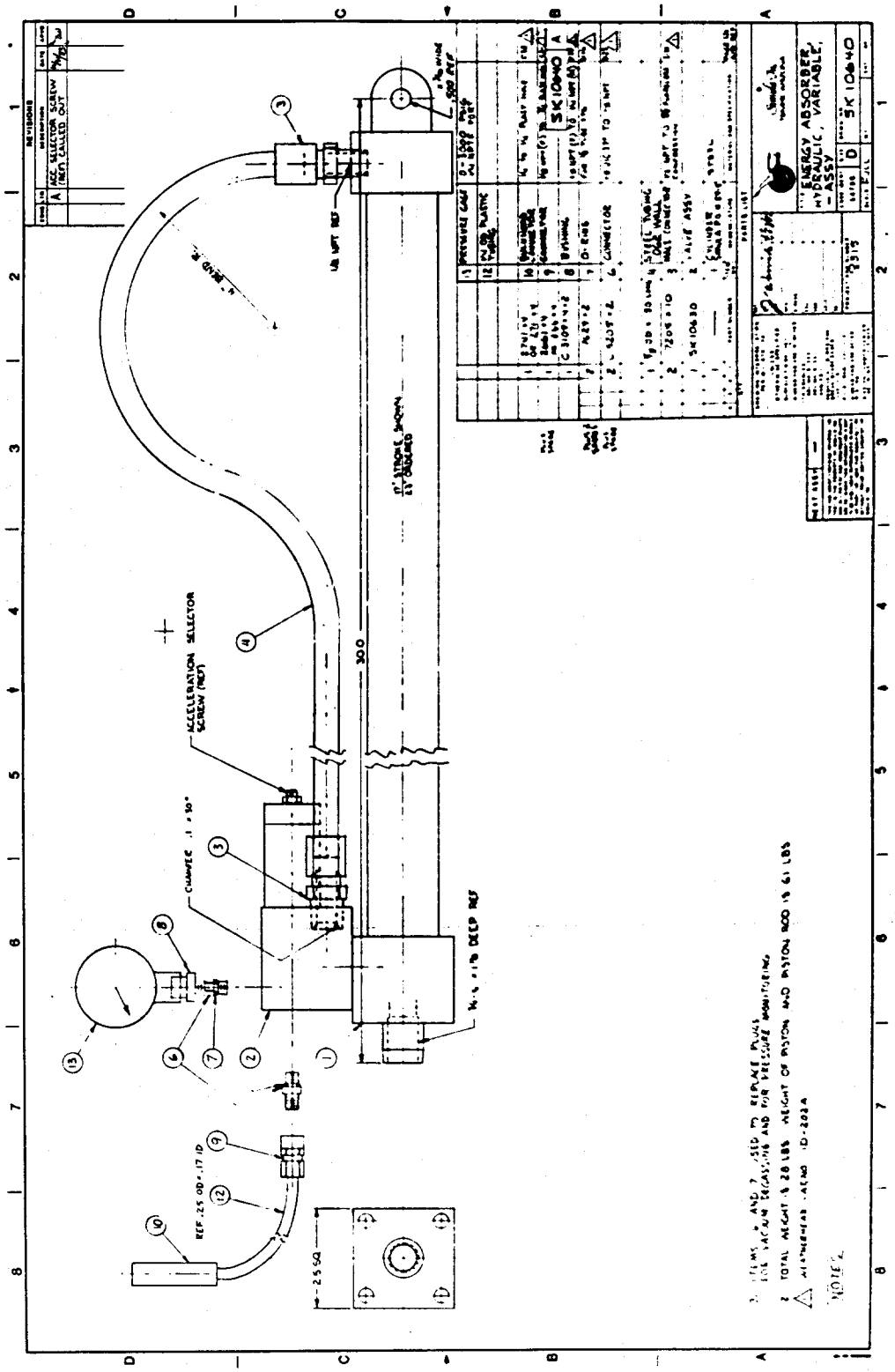
ENERGY ABSORBER, HYDRAULIC, VARIABLE, -ASSY
SK10640
SK10640-2
ACCELERATION SELECTOR SCREW (REF)
CHANGE .1 x 30°
300
REF .25 OD x .17 ID
2.550
N62269-82-C-0254

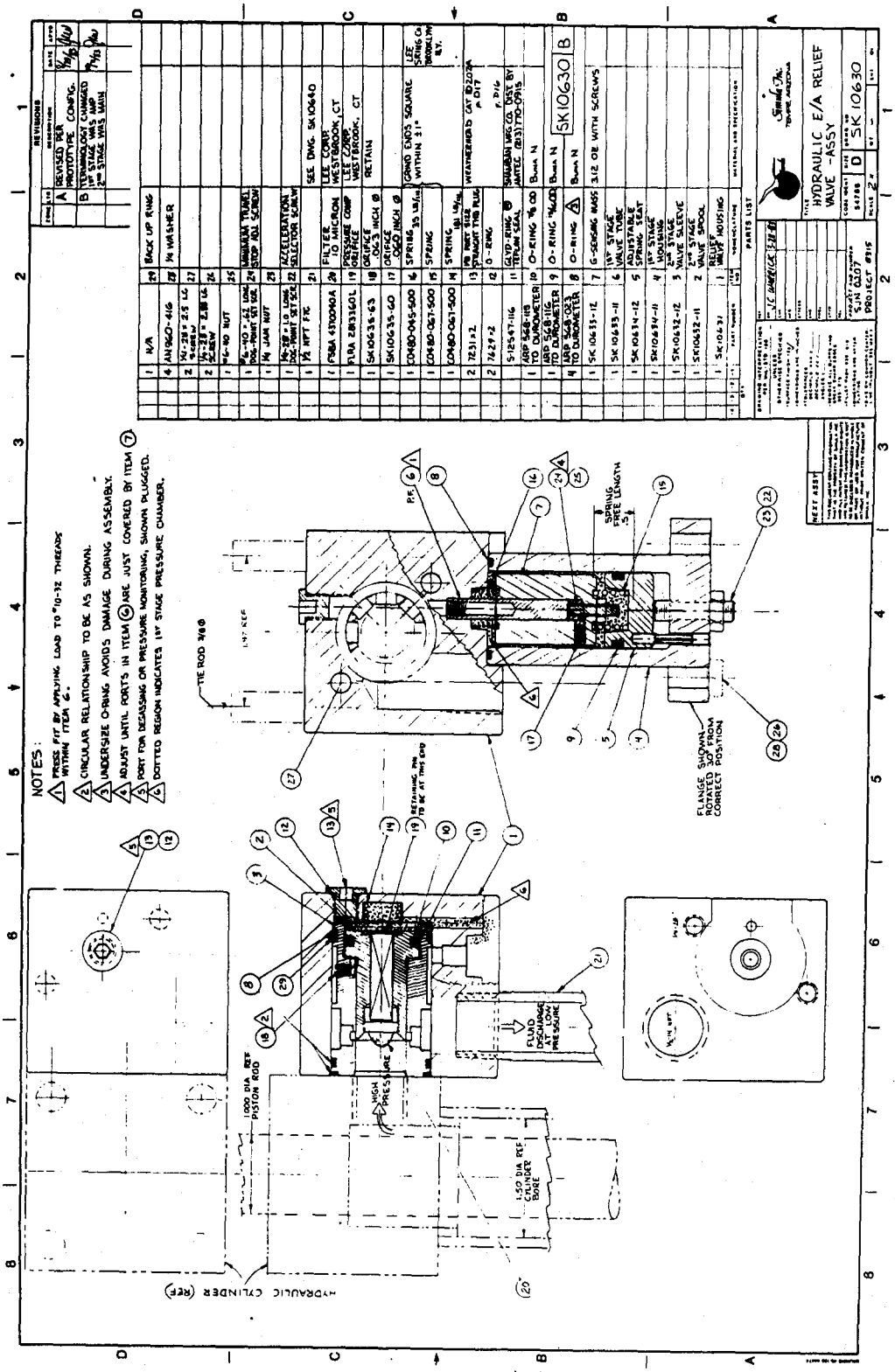

N62269-82-C-0254

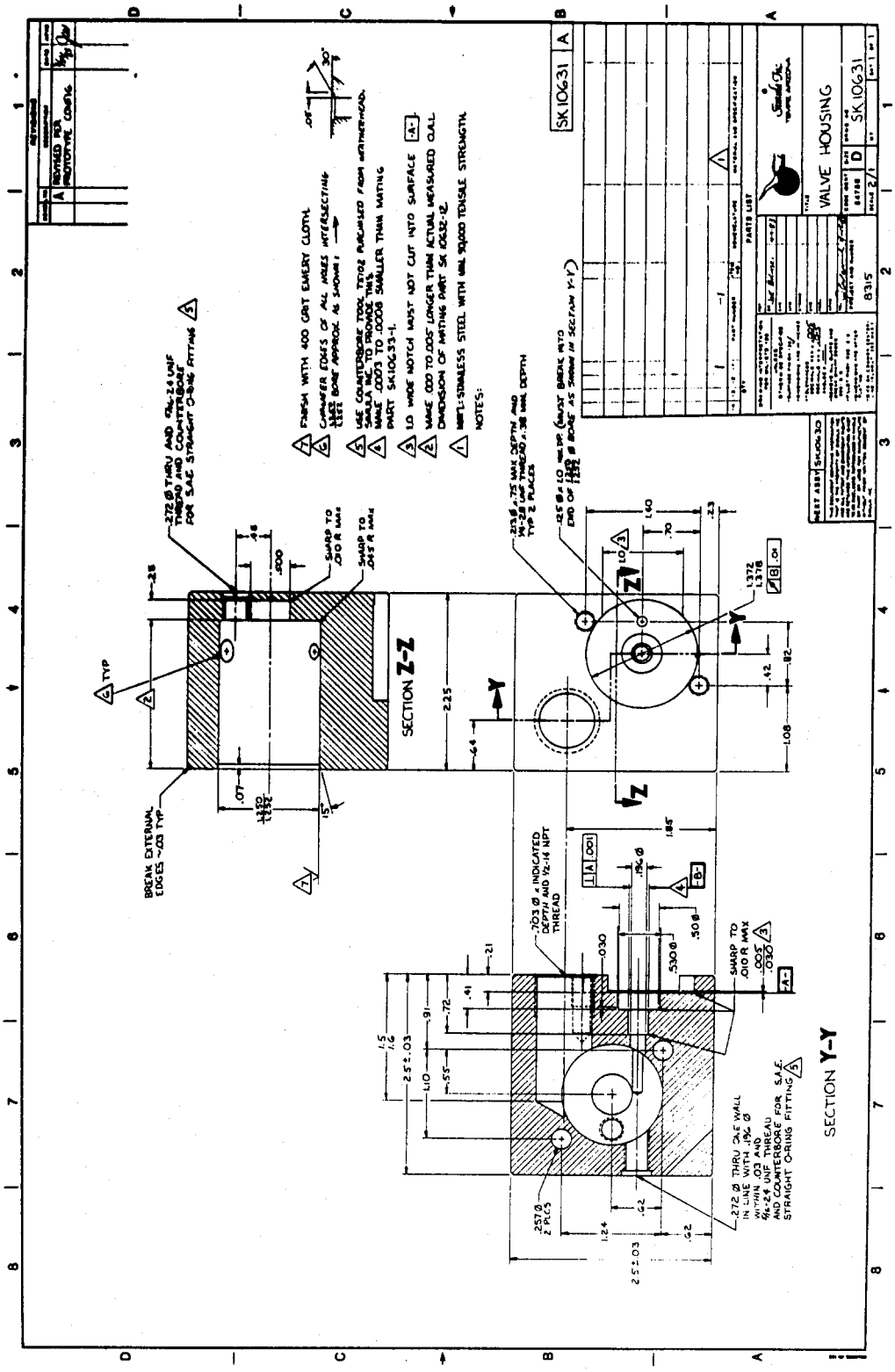

N62269-82-C-0254

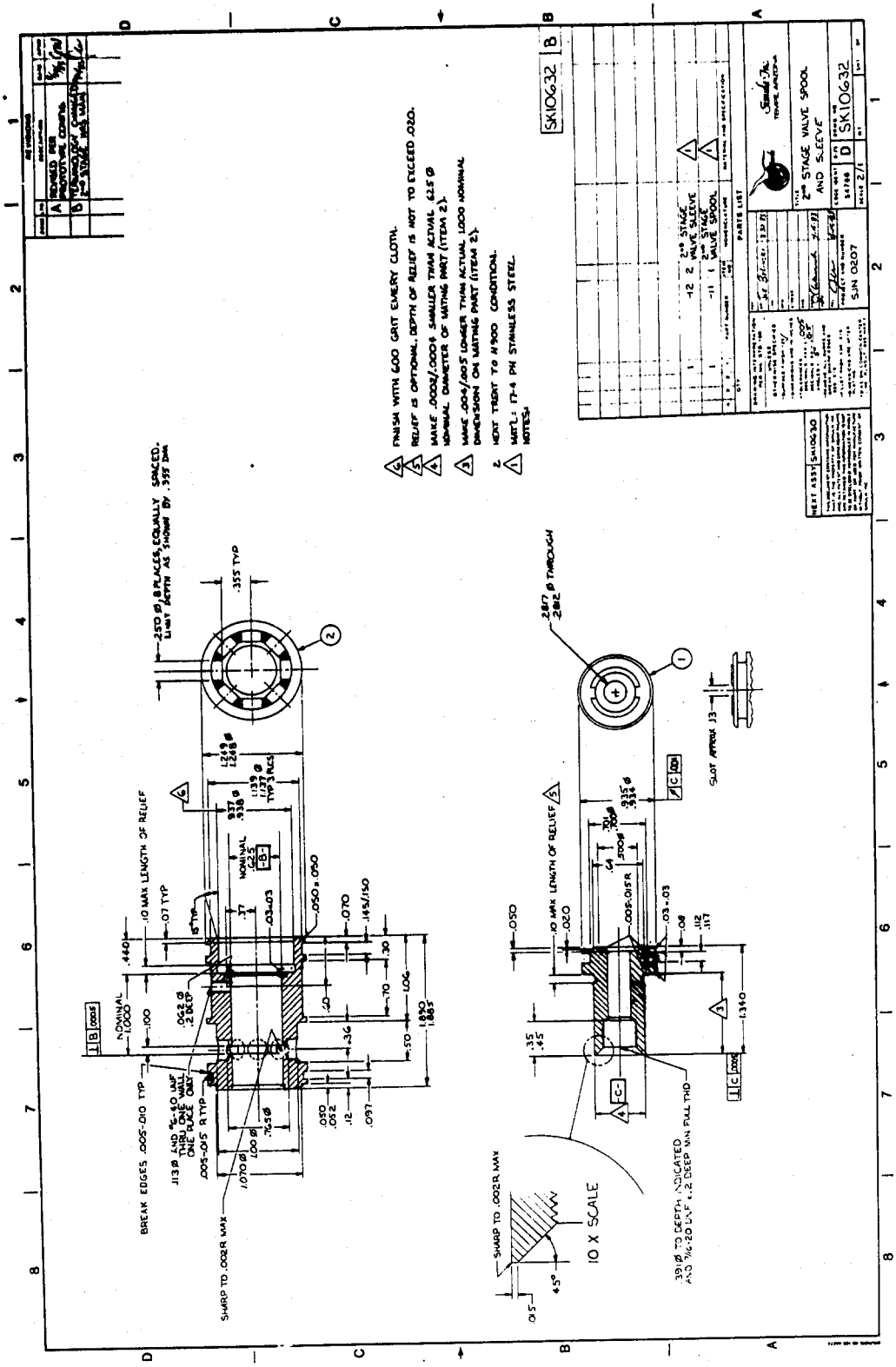

N62269-82-C-0254

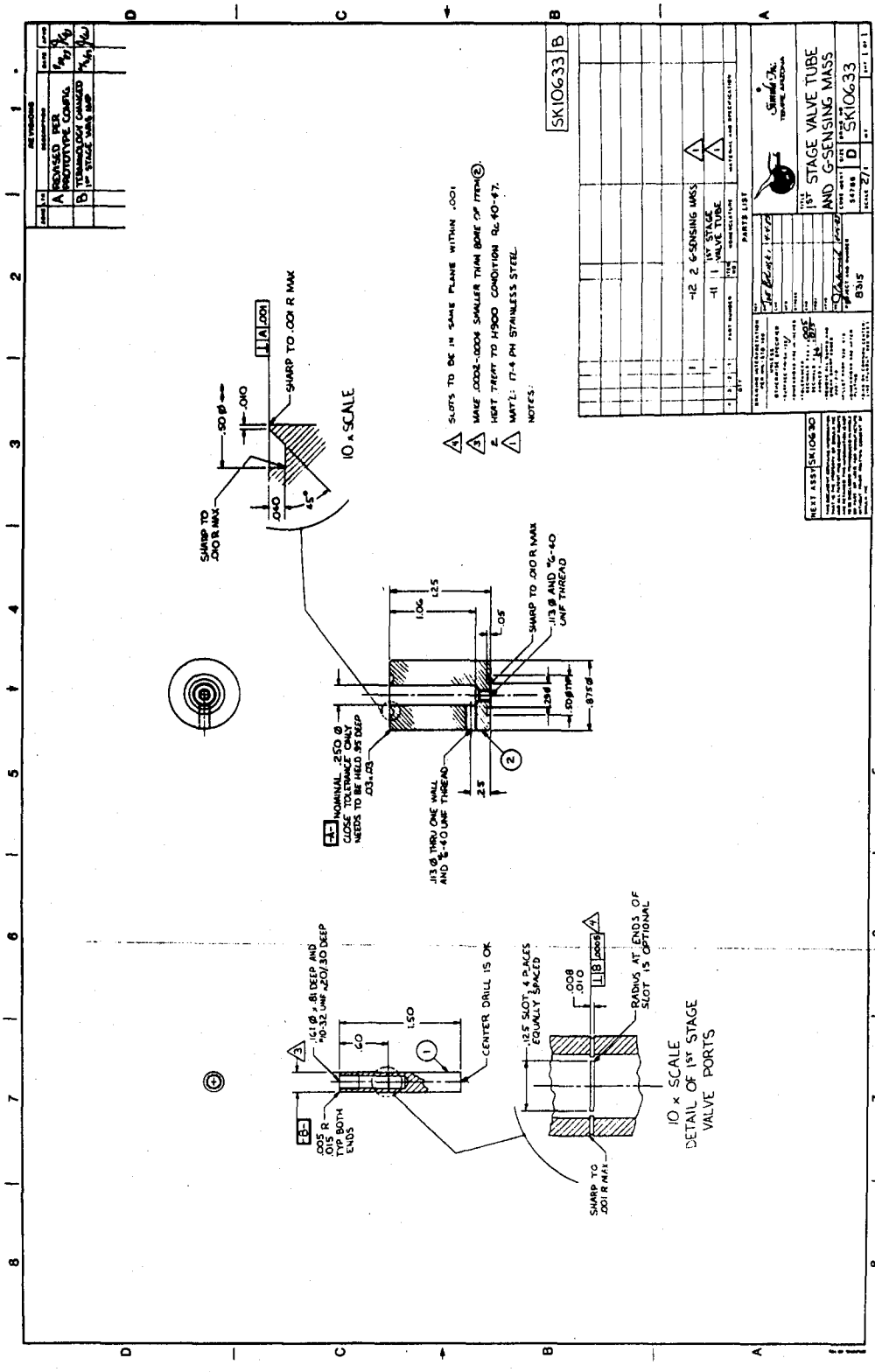
SK10633 B
1ST STAGE VALVE TUBE AND G-SENSING MASS
SK10633
10 x SCALE
DETAIL OF 1ST STAGE VALVE PORTS
10 x SCALE
SHARP TO .001 R MAX
SHARP TO .010 R MAX
SHARP TO .001 R MAX
.113 Ø AND 6-40 UNF THREAD
.113 Ø THRU ONE WALL AND 6-40 UNF THREAD
NOMINAL .250 Ø CLOSE TOLERANCE ONLY NEEDS TO BE HELD .05 DEEP .03 .05
CENTER DRILL IS OK
.161 Ø x .81 DEEP AND #0-32 UNF 4 DRILL 30 DEEP
.005 .015 R TYP BOTH ENDS
.125 SLOT, 4 PLACES EQUALLY SPACED
RADIUS AT ENDS OF SLOT IS OPTIONAL
SLOTS TO BE IN SAME PLANE WITHIN .001
MAKE .0023-.0004 SMALLER THAN BORE OF ITEM (2).
HEAT TREAT TO H900 CONDITION RC 40-47.
MAT'L: 17-4 PH STAINLESS STEEL.
NOTES:
-12 2 G-SENSING MASS
-11 1 1ST STAGE VALVE TUBE
PARTS LIST
N62269-82-C-0254

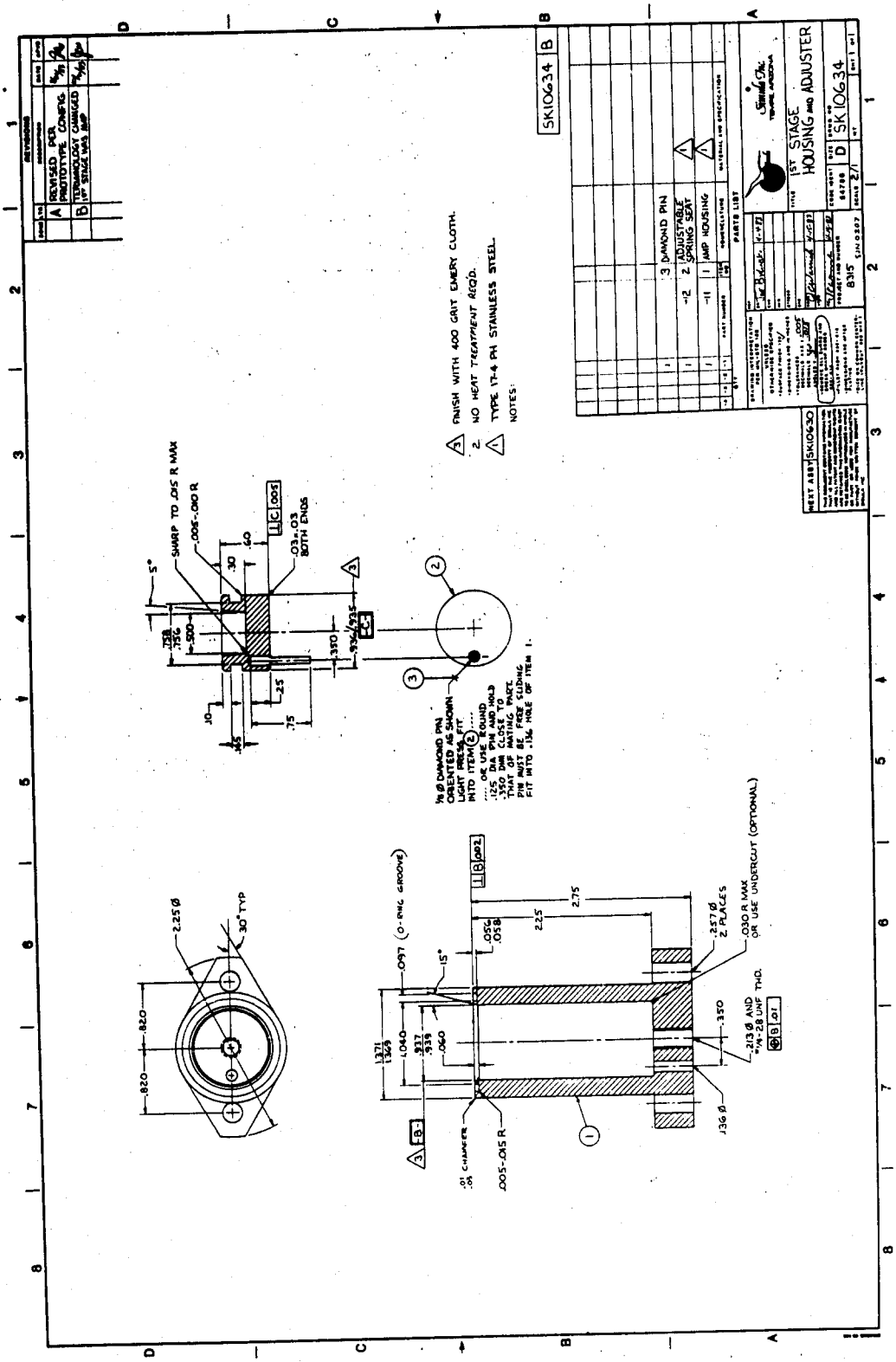

N62269-82-C-0254

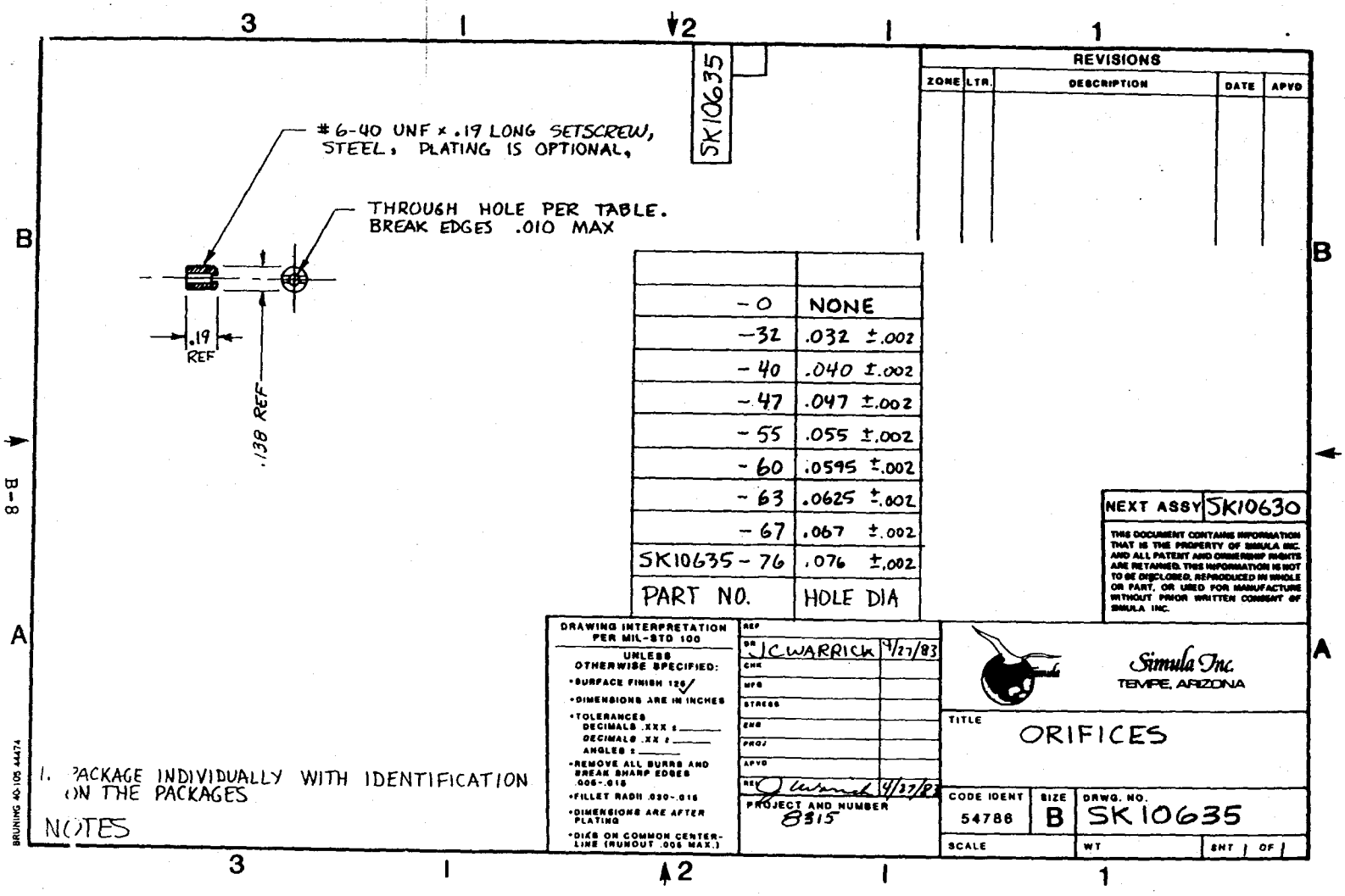

B-8

B-8

NADC-82025-60

N62269-82-C-0254